Harvested Energy Scavenging and Transfer capabilities in Opportunistic Ring Routing

JUNAID ANEES[1], **HAO-CHUN ZHANG**[1], **BACHIROU GUENE LOUGOU**[1],
SOBIA BAIG[2], **(Senior Member, IEEE), YABIBAL GETAHUN DESSIE**[1], **AND YIYI LI**[1]
[1]School of Energy Science and Engineering, Harbin Institute of Technology, Harbin 150001, China
[2]COMSATS University Islamabad, Lahore Campus, Lahore 54000, Pakistan

Corresponding author: Hao-Chun Zhang (hczhang@hit.edu.cn)

ABSTRACT Energy conservation has always been a prominent design goal for hierarchical routing protocols supporting sink mobility. Advertising the current position of mobile sink introduces control packet overhead which ultimately results in an increase in energy consumption and shorter network lifetime. Energy harvesting through ambient sources have enabled the utilization of rechargeable devices for Wireless Sensor Networks to perpetually remain operational. The modifications in the hierarchical structure of wireless sensor networks along with energy scavenging approaches could possibly minimize the control packet overhead and also provide a significant improvement in energy conservation. In this paper, we propose a novel Harvested Energy Scavenging and Transfer capabilities in Opportunistic Ring Routing protocol which uses a distinguishing approach of hybrid (ring + cluster) topology in which the network architecture is initially supported by the formation of a virtual ring structure and then a two-tier routing topology is used in the virtual ring as an overlay by grouping nodes into clusters. The rate of energy gain from solar harvesting and radio frequency transfer is the criterion for selecting cluster heads. The role of cluster heads is exploited to advertise the mobile sink current position as well as forward the aggregated data towards mobile sink using energy transfer based opportunistic routing. The simulation results reveal that our scheme considerably outperforms the existing benchmarks in terms of control packet overhead, energy conservation, network lifetime, packet delivery ratio and average end-end delay.

INDEX TERMS Clustering algorithms, energy harvesting, opportunistic routing, ring routing, routing protocols, wireless sensor networks.

I. INTRODUCTION

The existence of a mobile sink is based on the criticality and confidentiality of data in Wireless Sensor Networks (WSNs) i.e. critical data applications such as volcanic eruptions, forest fires or landslide detection will preferably have a static sink node but for applications involving critical and confidential data such as military, security and surveillance, mobile sink will always be preferred for data acquisition purposes in WSNs [1]–[4]. Mobile sink in WSNs can help in improving the network lifetime by ensuring load balancing across the network at the cost of problems like sink localization and high computational power. Previous studies have shown that the process of advertisement of sink node

position involves a huge control packet overhead if flooding mechanism is adopted as a communication broadcasting strategy [5]. Several multi-tier hierarchical routing protocols especially area-based routing protocols are proposed in literature to minimize this overhead. The high tier nodes in these hierarchical routing protocols acquire and store the updated sink position while low-tier nodes query the high-tier nodes to retrieve the updated position of mobile sink. This type of hierarchical routing protocol would result in the significant decrease of advertisement overhead and also enhance the energy efficiency. Although the overall energy consumption could be decreased in multi-tier hierarchical structure, there is a high possibility that high-tier nodes might face hotspot problems due to increased traffic [6]–[9].

Tunca *et al.* [10] proposed an area-based routing technique called ring routing, in which the formation of a virtual

ring shaped structure is used to store the information of sink node's current position. Greedy geographic forwarding mechanism is used to advertise the mobile sink current position and an anchor node is used to relay the data towards mobile sink. The quick accessibility of the virtual ring structure leads to faster data delivery in ring routing but at the cost of higher energy consumption and shorter network lifetime when anchor node is used for relaying data towards mobile sink. Instead of involving anchor node, if ring nodes are chosen to store the updated position of mobile sink as well as used for relaying the data towards mobile sink, the overhead will be reduced manifolds and the overall energy consumption can be decreased as well. Anees *et al.* [11] proposed delay aware and energy-efficient opportunistic node selection in restricted routing protocol for selection of next-hop using optimal path connectivity. Although these protocols are designed to support sink mobility but the problems like energy replenishment are not properly addressed. Recent advances have made it possible for sensor nodes to replenish their energy through scavenging such as solar, wind, thermal and kinetic harvesters etc. Furthermore, a lot of progress has been made in the development of wireless energy transfer mechanisms in which the energy is transferred from a sensor node to another node using radio waves [12]–[15].

Clustering is considered as one of the most popular techniques for traditional WSNs to achieve scalability and energy efficiency by reorganizing the nodes into disjoint clusters to form a two-tier network architecture. Each disjoint cluster includes one Cluster Head (CH) and several Cluster Members (CM). CH leads the cluster by collecting data from its CMs, thus constituting tier-1. For tier-2, we need to disseminate the collected data to Base Station (BS) from each cluster by forming an inter-CH topology [16], [17]. In the recent past, many clustering algorithms were developed in which a node (especially CH) cannot replenish its energy supply in a timely manner, thus becoming a bottleneck and leading to hotspot problem. In order to provide sufficient ambient energy to sensor nodes in the network using energy harvesters and transfer technologies, we need to redefine our strategy to maintain the WSNs. Besides, the residual energy of a sensor node, the rate of gaining ambient energy should also be considered before deciding the workload of a node. The overall network coverage should not be degraded because of different workload requirements of different nodes. Some nodes which require higher energy harvesting rate could be supported by an energy harvester and wireless energy transfer over Radio Frequency (RF) link. This imposes some new challenges at the network layer for which we need an additional management structure to support energy harvesting and energy transfer over RF [16]–[18].

Most published hierarchical routing algorithms have overlooked the problems in nodes closely located to mobile sink. In cluster-based routing, CHs closer to BS would forward more data packets to BS than other CHs, thus depleting their available energy at faster rate and degrading the overall network performance [18]. Some researchers suggested that

frequent clustering could resolve this unaddressed problem by rotating the role of CH among the CMs but the inherent traffic patterns will eventually affect all the nodes acting as CH if they are close to BS [16], [18]. In area-based routing like ring routing, the role of nodes in virtual ring which are responsible to store the updated position of the mobile sink, are rotated with the mobility of sink node but the likelihood of hotspot is still there due to single anchor node which is responsible to collect all the data packets from other nodes and forward them to mobile sink [11]. A possible solution could be to form multiple clusters in the virtual ring and provide sufficient amount of energy to CHs through energy harvesting and scavenging techniques. In this way, the mobility of sink node can be advertised through CHs without any interruption.

Furthermore, WSNs deployed in harsh environments are susceptible to interference which might result in opportunistic node connections due to link instability. Mobility in sink node also leads to opportunistic node connections due to intermittent links between sensor nodes. In addition to it, the node scheduling strategy such as asynchronous working-sleeping cycle is adopted by sensor nodes due to limited energy, thus leading to the possible existence of opportunistic node connections to achieve prolongation in network lifetime [19], [20]. Opportunistic Routing (OR) is defined as the scheme which involves 3 steps to select the next forwarder i.e. i) dynamic selection with reference to OR metric, ii) candidate selection algorithm, iii) candidate co-ordinate method. By utilizing the concept of opportunistic routing, sensor nodes can overhear their neighbor's transmission and create a set of potential forwarders using opportunistic connection random graph (OCRG) [21], [22]. Subsequently, the data forwarding takes place according to optimal link and path connectivity criteria.

The harvested energy can be treated as an alternative power source which could possibly increase the lifetime of connecting devices and make them self-sustainable. Solar energy harvesting is an affordable and clean source of energy that could resolve the impending energy replenishment problems in WSNs. For a viable solar power, developers should ensure the highest possible efficiency during daylight hours due to negligible energy harvesting during night hours. A typical solar harvesting system is based on the harvest-store and utilize system with different storage options like supercapacitors, batteries or a combination of two. For a typical outdoor illumination level of 500 W/m^2, we could achieve an efficiency between 15-25% for polycrystalline silicon but for an indoor illumination levels of 10W/m^2, efficiencies vary between 2-10% [23]. The deployment of solar harvesting depends on the type of application. Various examples of solar energy harvesting utilizing harvest-store-utilize architecture are: indoor router node, micro-scale indoor light energy harvesting system, battery less solar harvester, hydro watch and heliomote [23]–[26]. Another method for energy harvesting is RF-based energy harvesting in which radio waves are converted into DC power by utilizing single-stage or multi-stage
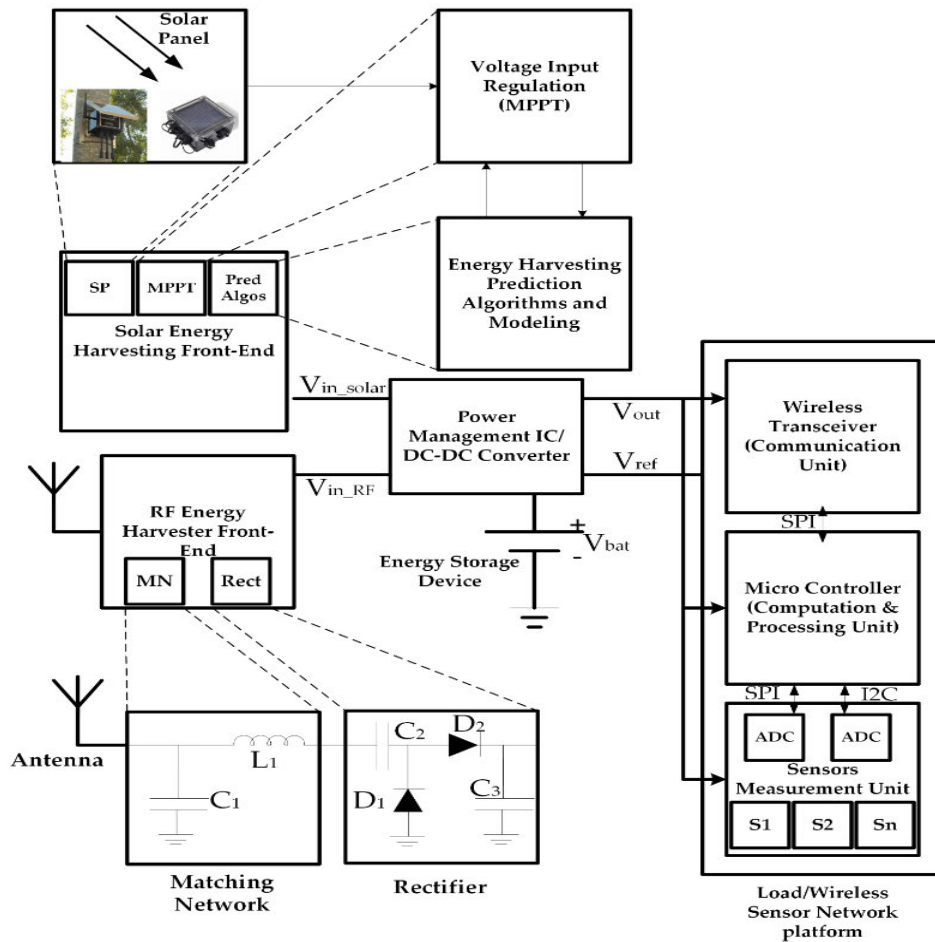
FIGURE 1. Solar and RF harvesting energy model for HESTOR.

approaches. The factors impacting the amount of RF energy harvested are source power, distance between source and BS, antenna gain and energy conversion efficiency. The typical RF to DC conversion efficiency is around 50-70% for an input power within 100m range. RF energy harvesting could be used in multiple ways, i) direct power (without energy storage), ii) supercapacitors, iii) battery-recharging, iv) battery activation. Examples of RF energy harvesting are power cast, wireless identification and sensing platform, contactless memories developed by STMicroelectronics, and TMS37157 developed by Texas Instruments [23], [27], [28].

We have considered a solar and RF energy harvesting design model for our scheme as shown in Fig 1. In this model, although solar and RF harvested energy are independent sources but they co-exist without significant interference. The solar energy harvesting front-end includes solar panels, voltage input regulators i.e. Maximum Power Point Tracker (MPPT) and energy harvesting prediction algorithms whereas the RF energy harvesting front-end includes antenna, matching network and rectifier. Both of the low-voltage signals are fed to Power Management Integrated Circuit (PMIC) or DC-DC converter. The high-voltage DC signal at

PMIC can be used to power the communication unit, microcontroller and sensor measurement units of WSN node. Since the power generated by the harvester can reach very low levels, it should be ensured that the PMIC operates with a high efficiency [23]–[26]. The DC-DC converter used in this design is boost converter which increases the amplitude of harvested energy by using capacitors, inductors and switch. In RF energy harvesting front-end, the RF antenna is used to capture the RF energy from the local environment and passes it to a matching network which ensures maximum RF to DC conversion efficiency. The rectifier then converts the RF signal into low-voltage DC signal and feds it to PMIC.

This article investigates the appropriate energy harvesting WSNs strategy for hybrid (area-based + cluster-based) opportunistic routing protocol with the objective of achieving stability, scalability and robustness in overall network operations to alleviate the problems of energy replenishment in nodes closer to mobile sink. We have proposed a novel, distributed, Harvested Energy Scavenging and Transfer capabilities in Opportunistic Ring routing (HESTOR) protocol. HESTOR pursues a hybrid (area-based + cluster-based) network architecture to achieve load balancing and

eliminate the hotspot problems. A virtual ring is formed in HESTOR to store the current position of mobile sink in which the role of each node is defined relative to virtual ring. Subsequently, a CH election take place in each cluster based on energy scavenging and energy transfer over RF links criterion after recognizing that nodes closer to sink consume more energy and require higher data rates.

We have critically analyzed the effect of different parameter settings to achieve desired topology in our extensive simulation. Several performance metrics such as control packet overhead, energy consumption in data transmission, network lifetime, Packet Delivery Ratio (PDR), average end-end delay, hop count, throughput along with different re-clustering epochs and sampling frequencies are considered for performance evaluation of HESTOR with other benchmarks. The rest of this paper is organized as follows. Section II covers the related research work. The system model is described in Section III. We have explained the detailed HESTOR architecture in Section IV. Packet overhead calculation is given in Section V. Simulation results of HESTOR are discussed in Section VI. Finally, Section VII concludes the paper.

II. RELATED RESEARCH WORK

Hierarchical routing protocols have been subject to various studies in the realm of WSNs. Several hierarchical routing protocols supporting sink mobility are reviewed in this section based on energy consumption and end-end delay. Tunca *et al.* [29] performed a comparative analysis of various hierarchical routing protocols supporting sink mobility i.e. i) Grid-based [6], [31]–[33], ii) Tree-based [7], [34]–[37], iii) Cluster-based [37]–[40], iv) Area-based [30], [9], [41]–[44] routing. Yarinezhad and Sarabi [32] proposed a virtual grid-based hierarchical routing protocol i.e., VGB which is designed to reduce the energy consumption and network delay by optimizing grid-header nodes while supporting sink mobility. One-hop away neighbors periodically store the updated position of mobile sink in VGB so that all sensor nodes can acquire that position information from them and forward the data to mobile sink using greedy geographic forwarding mechanism. Cardei and Yang [39] proposed a grid-based routing protocol supporting heterogeneous sensor networks. In this protocol, whole network area is divided into multiple grids. Each grid involves one super node which is employed to collect data from other members of the grid and deliver it to mobile sink. This heterogeneous grid-based protocol aims to achieve higher network lifetime with reduced hop count. The role of super node is quite similar to cluster heads in cluster-based routing protocols.

Han *et al.* [34] proposed Minimum Wiener index Spanning Tree (MWST) which is a tree-based hierarchical routing protocol to find the minimum spanning tree to decreased hop count between mobile sink and data generating node but the network lifetime is reduced when node density is increased due to data transmission dependency on specific sensor nodes. Anees *et al.* [45] developed an energy

efficient multi-disjoint path opportunistic node connection routing (EMOR) protocol for neighborhood area networks of Smart Grids. EMOR utilizes residual energy, buffer capacity, working–sleeping cycle of the sensor node and signal-to-noise ratio to calculate optimum link and path connectivity based on OCRG and spanning tree formation. The multi-disjoint path selection in EMOR helps to improve packet delivery ratio, network lifetime, end-end delay and total energy consumption. Habib *et al.* [43] proposed another tree-based hierarchical routing protocol offering faster data delivery, is known as Star Fish which comprises of a ring canal and multiple interconnecting canals to maintain the network backbone. Mobile sink position information is stored by ring canal and various interconnecting canals so that any data generating node can acquire the updated position of mobile sink from them. Mir and Ko [46] proposed a tree-based routing protocol involving a virtual tree structure in which the mobile sink updated position is advertised by root node to every leaf node. Maurya *et al.* [30] presented the Load based Ring Routing (LBRR) in which multiple agent nodes help in prolonging the network lifetime by selecting energy efficient next-hop during data transmission. Delay Aware and Energy-Efficient Ring Routing (DA-EERR) protocol is proposed by Maurya *et al.* [9]. DA-EERR adds the restricted search space to the concept of ring routing and LBRR to acquire minimum distance energy efficient next-hop node during data transmission. Anees *et al.* [11] proposed the Delay Aware and Energy Efficient Opportunistic node selection in Restricted Routing (DA-EEORR) for delay sensitive applications. In DA-EEORR, the mobile sink updated position information is advertised by multiple ring nodes instead of anchor nodes and data is forwarded to mobile sink using Ring nodes having maximum residual energy (RN_{maxRE}).

Cluster-based routing is a type of hierarchical routing protocols which leads to better energy utilization due to reduction of traffic overhead. Normally, we have a trade-off between energy consumption and network delay in cluster-based routing i.e. sensor nodes with high transmission power can communicate with mobile sink with less network delay but at the cost of higher energy consumption. However, sensor nodes with low transmission power can communicate with mobile sink with less consumed energy but at the cost of higher network delay. Afsar and Younis [18] proposed an unequal size clustering method known as CREST in which the probability of becoming CH in a cluster is based on a function of distance between BS and the node by employing track-based algorithms. Different approaches of Energy Harvesting Wireless Sensor Networks (EHWSNs) can be implemented for hierarchical routing protocols to benefit from the energy-harvesting properties of the WSNs. The differences between clustering algorithms in WSNs and EHWSNs include CH selection, CH rotation among cluster members, communication protocols between the cluster members and their assigned CH, communication protocols for inter-CH topology etc. Bozorgi *et al.* [47] discussed that the node harvesting rate and available energy are used to change the

CH election probability in EHWSNs clustering protocols. Zhang *et al.* [48] pointed out that selecting the optimum position of CH in a cluster also enhances the performance of EHWSNs as the CH position in a cluster directly affects the energy consumption of the overall cluster. Peng *et al.* [49] proposed an energy neutral clustering protocol based on scheduling the cluster members in a cluster to be CH for specific time slots to reduce the CH re-selection overhead in a cluster and to achieve a perpetual network operation. Li and Liu [50] proposed an optimization algorithm called Discrete Particle Swarm Optimization (DPSO) for optimum selection of CH in a cluster, which uses the EWMA algorithm to predict the energy harvesting rates of sensor nodes. Bai *et al.* [51] proposed Smart Energy Harvesting Routing (SEHR) in which a cost function is formulated based on the sent data type in addition to expected harvesting rate and the node's energy. The selection of route in SEHR is based on three strategies i.e. i) real-time power estimation of sensor node keeping in view the harvested energy and energy drain rate, ii) node mobility and stability, iii) prioritize routes based on the data type available. Martinez *et al.* [52] considered the waste of harvested energy and proposed Energy Harvesting Wastage Aware (EHWA) routing algorithm to select the best possible route by computing a cost function which is associated with the current battery level of a sensor node.

Padakandla *et al.* [53] investigated the optimal energy sharing policies in EHWSNs to maximize the network performance for the scenarios involving multiple sensor nodes and only one energy harvesting node. Prasad *et al.* [54] presented a detailed survey on various energy harvesting techniques especially covering topics such as power management and networking in EHWSNs. Varshney [55] proposed an emerging concept of simultaneous wireless information and power transfer (SWIPT) in which both energy and data are transferred over RF links simultaneously. Guo *et al.* [56] utilized the concept the SWIPT to extend the network lifetime of a clustered WSN by wirelessly charging the relay nodes which are responsible to share data with BS. Zhou *et al.* [57] proposed dynamic power splitting (DPS) to adjust the power ratio of information encoding and energy harvesting in EHWSNs. Furthermore, Lin *et al.* [58] used SWIPT in Body Area Networks (BANs) to simultaneously transfer the patient data and energy. It is pertinent to mention here that SWIPT can lead to an improvement in power consumption, transmission delay, spectral efficiency, and interference management as investigated by Perera *et al.* [59]. Hu *et al.* [60] pointed out that emerging communication technologies like cognitive radio networks (CRNs), full-duplex SWIPT systems, mobile data collection and secure data transmissions are using SWIPT. Overall, to the best of our knowledge, there is no published literature which factors in energy harvesting and scavenging while forming the data routes in ring routing. HESTOR introduces a hybrid (ring + cluster) architecture which utilizes the energy transfer based opportunistic routing algorithm to solve the mobile sink position

advertisement and hotspot problems while enabling a unified routing framework for both data and energy.

In this article, we have proposed novel, distributed HESTOR scheme which is a hybrid (ring + cluster) energy harvesting opportunistic routing protocol designed to efficiently handle the hotspot problems due to energy replenishment and advertisement of mobile sink position while achieving idiosyncratic performance in terms of control packet overhead, energy consumption, PDR, average end-end delay, network lifetime and throughput. Although both DA-EEORR and HESTOR use optimal link and path connectivity calculations based on asynchronous working-sleeping cycle strategy of sensor nodes, the difference between RNs in DA-EEORR and CHs in HESTOR can be explained in terms of energy harvesting and scavenging abilities. The selection of CH in each cluster is based on available battery energy, harvested energy using solar and wirelessly transferred energy using RF links in HESTOR whereas the RN_{maxRE} selection in DA-EEORR is totally based on maximum residual energy i.e. available battery energy which leads to higher status transitions in sensor nodes, thus reducing PDR & network lifetime while increasing the control packet overhead and end-end delay. The comparison between HESTOR and contemporary routing protocols in terms of heterogeneity, virtual structure, energy-efficiency, multiple sink support, load-balancing, data aggregation, control packet overhead and average end-end delay is given in Table 1.

III. SYSTEM MODELING

A *MxM* network area is considered for HESTOR in which *N* sensor nodes are deployed randomly and independently. Mobile sink can randomly move in the network at any time for data acquisition. We have assumed that sensor nodes follow a uniform random distribution. All sensor nodes use short radio range (R_S) for sensing and transmission purposes whereas mobile sink can use R_S for transmission & reception and long radio range (R_L) for data collection tasks using a tag message. The inner radius (*IR*) and outer radius (*OR*) of the mobile sink can be determined using the assumption that both inner and outer radius of circles of mobile sink have the same area (based on the concept of uneven tracking) i.e.

$OR = \sqrt{2I}R$. However, all sensor nodes can exploit the power control function and communicate with different neighboring nodes within various power levels. Furthermore, we have assumed that all sensor nodes are equipped with a rechargeable battery and an energy harvester, e.g., a solar cell. For example, Nickel Metal Hydride (NiMH) battery with a maximum capacity of 2500mAh and efficiency of about 0.66 or Lithium ion battery with a maximum capacity of 2500mAh and charge/discharge efficiency of 80-90 %. Each sensor node is equipped with a power splitting radio, which is composed of a signal processing unit and an energy harvesting unit to transfer energy from neighbors using RF link based on Relative Signal Strength Indicator (RSSI). It is also assumed that every sensor node is aware of its position using the energy-efficient localization method [61]–[64] and

TABLE 1. Comparison of various hierarchical mobile sink routing techniques with HESTOR.

Routing Protocol	Virtual Structure	Heterog-eneity	Multi Sink	Mobility pattern	Energy Efficiency	Load Balancing	End-End Delay	Data Agg	Protocol overhead
VGB	Grid	No	Yes	Random	Less	Balanced	Smaller	No	Average
MWST	Tree	No	Yes	Random	Less	Low	Moderate	Yes	Low
Star Fish	Ring & Fishbone	No	No	Random	Less	Balanced	Smaller	No	Average
DSDRO	N/A	No	No	Predefined	More	Balanced	Moderate	No	Average
ENCP	Cluster	No	No	Random	More	Balanced	Larger	No	Average
DPSO	Cluster	No	No	Random	More	High	Smaller	Yes	Average
EHWA	Cluster	No	No	Random	More	High	Moderate	No	High
Ring Routing	Ring	No	No	Random	Medium	Balanced	Smaller	No	Average
LBRR	Ring	Yes	No	Random	Less	High	Larger	No	Average
EMOR	Tree	Yes	Yes	Random	More	High	Moderate	No	Average
DA-EERR	Ring	Yes	No	Random	Medium	High	Moderate	Yes	Average
DA-EEORR	Ring	Yes	No	Random	More	Balanced	Moderate	Yes	Low
HFECS	Cluster	Yes	No	Random	High	Balanced	Moderate	Yes	Low
HESTOR	Cluster & Ring	Yes	No	Random	High	Balanced	Smaller	Yes	Average

the distance between the sensor node and mobile sink can be estimated using RSSI. Moreover, the simplified energy consumption model [65] for radio energy dissipation during transmission and reception is considered in which the energy required to transmit l bits of data over distance d can be given in (1) as:

$$E_{Tx}\left(V_i, V_j\right) = \begin{cases} E_{elec}l + \varepsilon_{fs}ld_{V_iV_j}^2 & d < d_0 \\ E_{elec}l + \varepsilon_{mp}ld_{V_iV_j}^4 & d \geq d_0 \end{cases} \quad (1)$$

where E_{elec} is the energy spent by transmitter on running the radio electronics, ε_{fs} is the free space energy dissipated by power amplifier depending on the Euclidean distance $d_{V_iV_j}$ between the transmitter and receiver, ε_{mp} is the muti-path fading factor for energy dissipated by power amplifier depending on Euclidean distance $d_{V_iV_j}$ between transmitter and receiver. The threshold distance d_o is given as $d_o = \sqrt{\varepsilon_{fs}/\varepsilon_{mp}}$. Likewise, the energy required to receive l bits of data over distance d is given in (2) as:

$$E_{Rx} = E_{elec}l \quad (2)$$

The energy used for sensing l bits of data in the virtual ring at the beginning of each round can be given as $E_{sense} = E_{elec}l$. Accordingly, the total energy consumed by

cluster member (CM) can be computed in (3) as:

$$E_{CM} = E_{sense} + E_{Tx} = E_{elec}l + E_{elec}l + \varepsilon_{fs}ld_{V_iV_j}^2 \quad (3)$$

We also know that each CH is responsible for data gathering, aggregating the received data and then relaying that data towards mobile sink, so the total energy consumed by a CH can be computed in (5) as

$$E_{CH} = E_{sense} + \left(\frac{N_{VR}}{N_C} - 1\right)E_{Rx} + \left(\frac{N_{VR}}{N_C}\right)lE_A$$
$$+ \left(\frac{N_{VR}}{r}\right)E_{Tx} \quad (4)$$

$$E_{CH} = E_{elec}l + \left(\frac{N_{VR}}{N_C} - 1\right)E_{elec}l + \left(\frac{N_{VR}}{N_C}\right)l\frac{E_{elec}}{R_{CC}}$$
$$+ \left(\frac{N_{VR}}{r}\right)E_{elec}l + \left(\frac{N_{VR}}{r}\right)\varepsilon_{mp}ld_{V_iV_j}^4 \quad (5)$$

where N_C symbolizes the number of clusters in the virtual ring, $\frac{N_{VR}}{N_C}$ is the number of CNs or RNs per cluster in which we have 1 CH and $\frac{N_{VR}}{N_C} - 1$ CMs. E_A signifies the data aggregating energy at CH level, r represents the compression ratio and R_{CC} symbolizes the communication to computation ratio. Table 2 summarizes the notations used in this paper.

TABLE 2. Notation description.

Notation	Meaning	Notation	Meaning
E_{Tx}	Energy required to transmit l bits of data over distance d	R_L	Long-radio range
E_{Rx}	Energy required to receive l bits of data over distance d	W_v/S_v	Working/Sleeping schedule
$E_{trans(V_j,V_i)}$	Amount of energy node j can transfer to node i	F_{ST}	Status transition frequency
η	Energy conversion efficiency	$TF_{V_iV_j}$	Time-Frequency parameter
μ	Energy and data splitting ratio	$E_{C(V_i,V_j)}$	Energy consumed over link (i,j)
h	Channel gain	Γ_{V_i}	Node's gain degree
β_1	Constant for radio propagation properties of the environment	$E_{Harv(V_i)}$	Harvested energy of a node
α_1	Path loss exponent		
E_{elec}	Energy spent for running radio electronics	$E_{Bat(V_i)}$	Remaining battery energy of a node
l	Number of bits	E_T	Total available energy of a node
$d_{V_iV_j}$	Euclidean distance b/w transmitter and receiver	t_T	Threshold time for CH competition
ε_{fs}	Energy dissipation in free space fading	$L_{V_iV_j}$	Link connectivity of V_i & V_j
ε_{mp}	Energy dissipation in multi-path fading	$LC_{E(V_i,V_j)}$	Data routing cost
N	Number of sensor nodes	$PC_{V_iV_j}$	Path connectivity of V_i & V_j
N_C	Number of clusters	EOH	Expected Optimal Hop
E_{sense}	Energy consumed during sensing	Q	Expected Optimal Hop Average
E_A	Energy consumed during aggregation	α	Weights for $TF_{V_iV_j}$ and $LC_{E(V_i,V_j)}$
r	Compression ratio	I_R	Inner radius of mobile sink
R_{CC}	Communication–Computation ratio	O_R	Outer radius of mobile sink
E_{CH}	Energy consumed by cluster head	T_{CP}	Data Collection period
E_{CM}	Energy consumed by cluster member	N_{VR}	Number of nodes in virtual ring
$E_{cluster}$	Energy consumption of a cluster	$E_{virtual\ ring}$	Energy consumed in virtual ring
R_S	Short-radio range	R_C	Cluster range

IV. DETAILED HESTOR ARCHITECTURE

In this section, the architecture of HESTOR is discussed in detail. If the nodes are located inside R_S or outside R_L, they are imposed to perform the role of normal node (NN) but if the nodes are located outside R_S and inside R_L, then they are imposed to perform the role of candidate node (CN) or Ring node (RN). Mobile sink launches data collection by broadcasting a tag message containing the mobile sink address and data collection duration. Sensor nodes calculate their working-sleeping cycle keeping in view the data collection duration of mobile sink. Subsequently, each sensor node broadcasts a probe message containing source address, broadcast address, node role, working-sleeping schedule, neighbors address and Expected Optimal Hop (EOH) [45]. The design of HESTOR is segmented into four different sections; (i) Construction of virtual ring, (ii) Virtual ring CH election, (iii) Energy transfer based opportunistic routing, (iv) Network maintenance.

A. CONSTRUCTION OF VIRTUAL RING

After defining different nodes' roles with respect to their position in the network, mobile sink selects a two-hop away node as Starting Ring node (SRN) based on its highest energy. SRN creates Ring Creation Token (RCT) and announces its role to other CNs to make a closed virtual ring between inner radius (I_R) and outer radius (O_R) of mobile sink. I_R and O_R of mobile sink are defined in the same context as R_S and R_L. The selection criterion for choosing the next CN is to check if it makes a maximum angle with the solid virtual line of mobile sink. In counter clockwise direction, SRN forwards

the RCT to that CN which fulfills this criteria. When a CN receives RCT from a neighbor, it changes its role to RN and then follows the same criteria to forward the RCT to its neighbor in counter clock wise direction. This process continues until RCT is being received by SRN from a recently appointed RN, thus leading towards the formation of a closed virtual ring around mobile sink. The illustration of virtual ring structure and RCT forwarding mechanism can be seen in Fig 2-4.

In HESTOR, the relationship of link connectivity in terms of asynchronous working-sleeping cycle and total available energy should be clearly explained before discussing virtual ring CH election and energy transfer based opportunistic routing. Fig 5 depicts the link connectivity between adjacent nodes with respect to total energy available (including harvested energy, battery energy and RF transfer energy) and asynchronous working–sleeping cycle of sensor nodes. Each of the nodes have different energy management status and working-sleeping cycle. According to energy management status, node V_i and V_j (active state) can communicate with each other and node V_k (charging state) due to existence of opportunistic node connection in timeslot t1-t2. Another opportunistic node connection exists in timeslot t2-t3 where nodes V_i and V_j (active states) can communicate with node V_k (entering active state). When a node is in working mode especially at night, its residual energy starts declining rapidly due to unavailability of solar energy harvesting, so the charging and discharging energy cycle of sensor nodes can be adjusted in accordance with the application requirements.
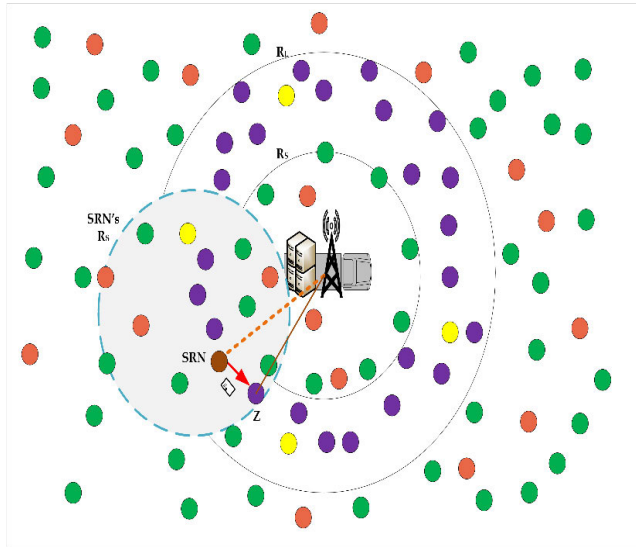
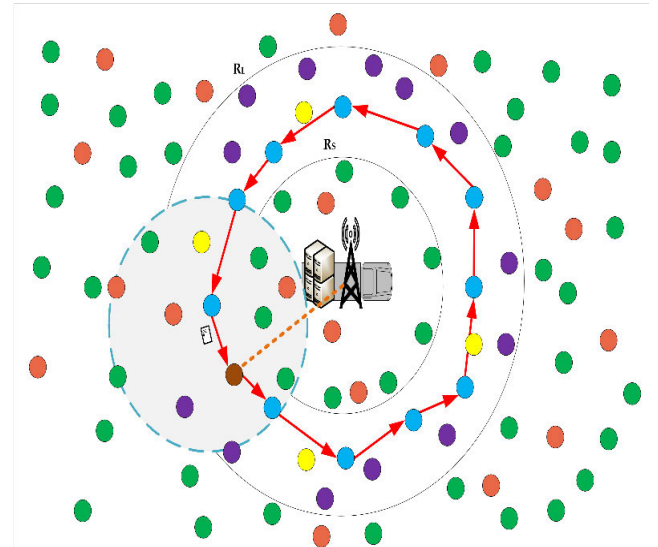**FIGURE 2.** Announcement of SRN role after creation of RCT.

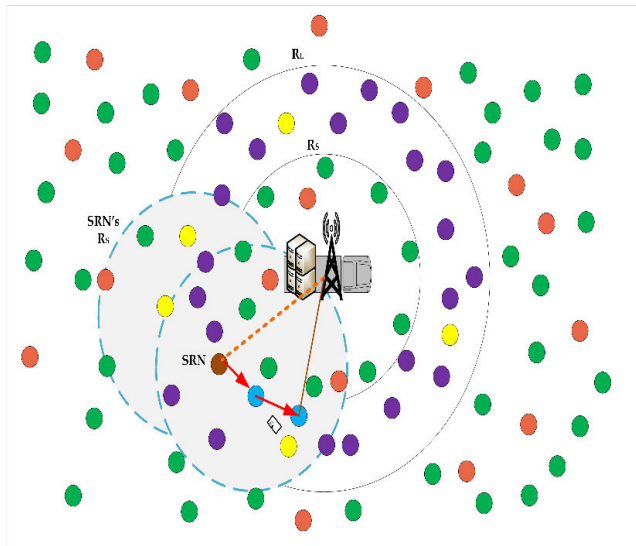**FIGURE 4.** Completion of virtual ring.

FIGURE 3. First RN chooses the appropriate CN for forwarding RCT.

B. VIRTUAL RING CH ELECTION

Once all the nodes are aware of their roles and the formation of virtual ring is ensured, the competition for CH election in the virtual ring starts. HESTOR uses a competition-based CH election in the virtual ring, where the most qualified RN among the CH candidates are picked by mobile sink to be selected as CHs. Keeping in view the energy transfer mechanism through RF transfer, our selection criteria for CHs in the virtual ring is based on node's gain degree. Initially the mobile sink select those RNs whose sum of harvested energy and battery energy is greater than the rest of cluster members. Then mobile sink sends CH_Election_message to those RNs. Each potential CH after receiving the CH_Election_message sends the CH_Announce_message to neighboring RNs and CNs. RNs or CNs receive the CH_Announce_message

and send the connection request message (Con_Req) to nearest CH. Subsequently, the CHs receives the Con_Req from multiple potential CMs, creates a cluster_member_set (CM_set) and adds all potential CMs to CM_set. In order to understand the concept of node's gain degree, we recall that sensor nodes in a cluster can control their power levels and communicate with neighbors placed at different locations while reducing their maximum transmission range according to cluster size. The amount of energy a node i could receive from its neighbor j through RF transfer such that $d_{i,j} \leq R_C$ can be defined as:

$$E_{trans(V_j, V_i)} = \eta \mu P_j |h_{V_i, V_j}|^2 = \eta \mu P_j |\beta_1 d_{(V_i, V_j)}^{-\alpha_1}|^2 \quad (6)$$

$$\Gamma_{V_i} = \sum_{j=1}^{k} E_{trans(V_j, V_i)} = \sum_{j=1}^{k} \eta \mu P_j |\beta_1 d_{(V_i, V_j)}^{-\alpha_1}|^2 \quad (7)$$

where $E_{trans(V_j, V_i)}$ is the amount of energy node j can transfer to its neighbor i, η is the energy conversion efficiency for which the condition is $0 < \eta < 1$, μ is the energy and data splitting ratio for which the condition is $0 < \mu < 1$, P_j is the signal power received from node j, and the channel gain $h_{V_i, V_j} = \beta_1 d_{(V_i, V_j)}^{-\alpha_1}$, where β_1 is a constant which depends on the radio propagation properties of the environment, and α_1 is the path loss exponent, Γ_{V_i} is the node V_i's gain degree which depends on the RF energy transfer from j neighbors in (6) and (7). Furthermore, the total available energy at node i can be computed as:

$$E_{T(V_i)} = \Gamma_{V_i} + E_{Harv(V_i)} + E_{Bat(V_i)} \quad (8)$$

where $E_{Harv(V_i)}$ is the harvested energy of node i using its own solar energy harvester, $E_{Bat(V_i)}$ is the remaining battery energy of node i in (8). All the nodes within the cluster multi-cast an energy_req_message which includes E_{trans} and source address of the node. Each node in the cluster calculates its E_T after every threshold time t_T. The threshold time t_T depends
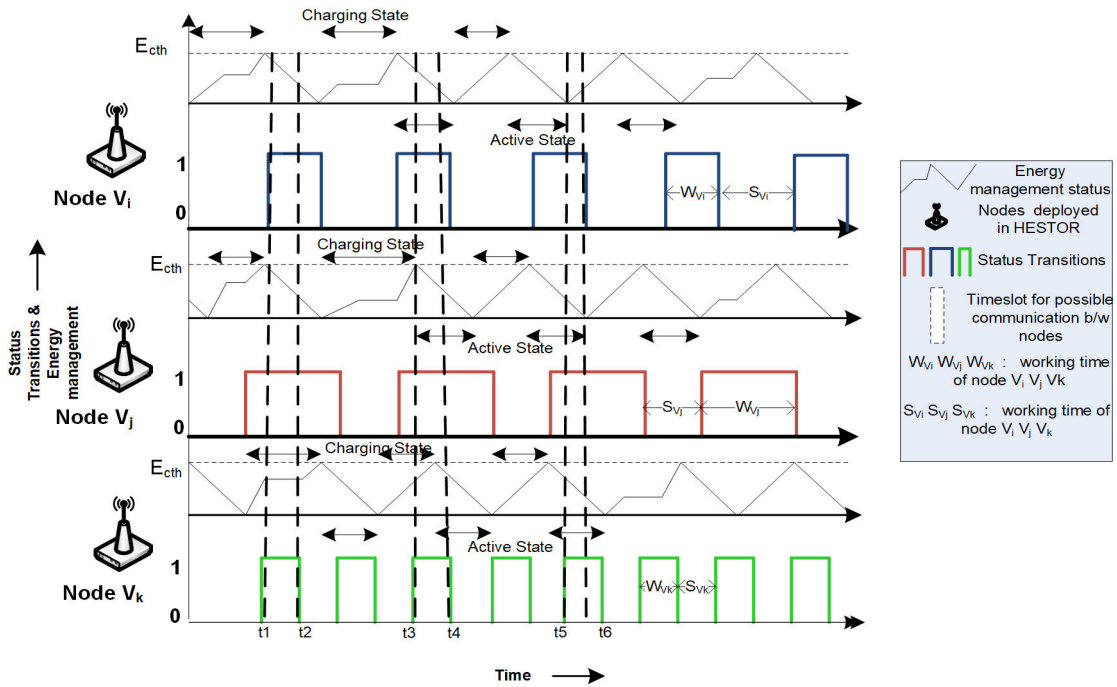
FIGURE 5. Relationship between link connectivity of adjacent nodes and their different energy management status.

on the duration of the CH competition and node density in the virtual ring. The node with highest E_T in each cluster wins the CH competition and is declared as CH. Foregoing in view, CH in each cluster perform tasks such as (i) relaying the data from nodes in O_R to nodes in I_R and further to mobile sink (ii) processing data aggregation request and reply packets from the data generating nodes in O_R. It is pertinent to mention here that the amount of energy a node share with its neighbors depends on node activity such as sensing, relaying, working-sleeping schedule etc. We suppose a continuous time between t1 and t2 for the energy consumption measurement. Residual energy in time t is defined by omitting consumed energy in Δt from the initial battery and harvested power in t-Δt. Thus, the energy efficiency for HESTOR can be computed in (9) as:

$$Eresidual(t) = Einitial(t - \Delta t) - Econsumed(\Delta t) \quad (9)$$

$$Eeff = (Eresidual/Einitial) \times 100$$
$$= (Einitial(t - \Delta t) - Econsumed(\Delta t))$$
$$/Einitial(t - \Delta t)) \times 100 \quad (10)$$

where $Einitial (t - \Delta t) = ET$, so our energy efficiency will become,

$$Eeff = (ET - Econsumed(\Delta t))/ET \times 100. \quad (11)$$

The virtual ring CH election process can be illustrated from Fig 6. The CH Election process is summarized in Algorithm 1 and 2.
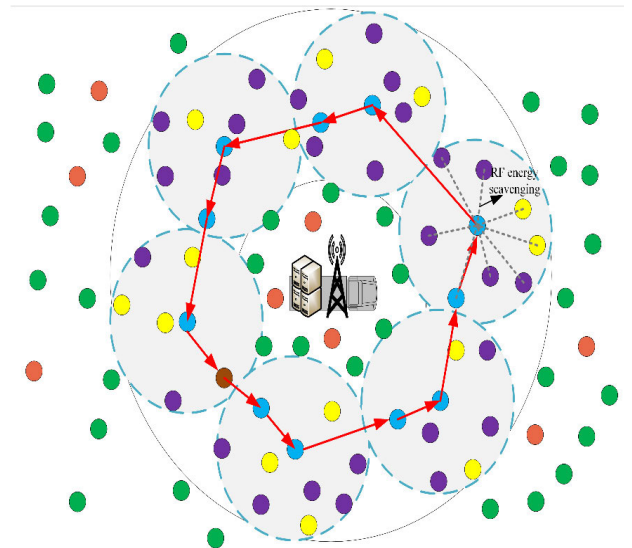

FIGURE 6. Virtual ring CH election.

C. ENERGY-TRANSFER BASED OPPORTUNISTIC ROUTING
In our proposed scheme, routing topology serves both data and energy dissimilar to two-tier conventional WSNs. We have provided an additional structure in HESTOR for factoring in the role of wireless energy transfer in routing topology at the cost of some overheads. Furthermore, we designed our proposed scheme using opportunistic connection random graph (OCRG). Let's denote our OCRG by a graph G (V,E,L) in which V represents the set of nodes in the network, E represents set of opportunistic connections

---

Algorithm 1 HESTOR CH Election (CH Side)

Input: Mobile sink selects the potential RNs for CH competition within virtual ring

Output: CH decision

Begin:

1. **if** (CH_Election_message received && $C_R = 1$), **then**
2. Store the current position of mobile sink in its local buffer
3. Start preparing CH_Announce message in order to advertise your role as potential CH in the cluster
4. Send CH_Announce message to neighboring RNs and CNs
5. **if** (Con_Req message is received from potential CMs), **then**
6. V_{CH} creates a cluster member set, i.e., CM_set
7.   Add the potential CMs to CM_set
8. **else** Wait till the Con_Req message is sent by potential CMs
9. **end if**
10. **else if** (CH_Election_message received with CM_set $\neq \emptyset$ && $C_R > 1$), **then**
11. V_{CH} multicasts the energy_req_message to its CMs
12. Compute E_T in terms of energy transfer over RF, harvested energy and battery energy
13. **for** each $V_{CM(i)}$ in a cluster, **do**
14.   **if** (V_{CH}'s $E_T \geq$ $V_{CM(i)}$'sE_T), **then**
15. V_{CH} sends CH_Announce message to each CM in the next round
16.   **else if** (V_{CH}'s $E_T <$ $V_{CM(i)}$'sE_T), **then**
17. V_{CH} sends CH_Election_message to $V_{CM(i)}$
18. $V_{CM(i)}$ sends CH_Announce message to each CM
19.   **end if**
20. **end for**
21. **end if**

Algorithm 2 HESTOR CH Election (CM Side)

Input: Mobile sink selects the potential RNs for CH competition within virtual ring

Output: Executing all tasks relevant to CM after CH election procedure

Begin:

1. **if** (CH_Announce_message received from a potential V_{CH} && $C_R = 1$), **then**
2. Send the Con_Req to that V_{CH}
3. **else** Wait till the CH_Announce message is received from a potential V_{CH}
4. **end if**
5. **if** ($C_R > 1$), **then**
6. V_{CM} multicasts the energy_req_message to its neighbors
7. Compute its E_T based on energy transfer over RF, harvested energy and battery energy
8. **for** each $V_{CM(j)}$ in a cluster, **do**
9.   **if** ($V_{CM(i)}$'s $E_T >$ $V_{CM(j)}$'sE_T && $V_{CM(i)}$'s $E_T >$ V_{CH}'sE_T), **then**
10. $V_{CM(i)}$ sends CH_Announce message to $V_{CM(j)}$ and V_{CH}
11.   **else if** ($V_{CM(i)}$'s $E_T <$ V_{CH}'sE_T ||$V_{CM(i)}$'s $E_T <$ $V_{CM(j)}$'sE_T) , **then**
12.   Wait till the CH_Announce message is received from new V_{CH}
13.   **end if**
14. **end for**
15. **end if**

---

existing between any two adjacent neighbors and L represents the link connectivity of any two adjacent nodes in set V. The link connectivity is dependent on factors like data routing cost and asynchronous working–sleeping cycle of sensor nodes. The longer the node's working time, more likely it will communicate with adjacent nodes and higher the status transition frequencies of nodes, more likely it will contribute to improve the link connectivity. Each direct link between adjacent sensor nodes has a data routing cost $LC_E: E \rightarrow R$ such that $LC_E(i, j)$ is the cost associated with link (i,j). Our routing metric can be defined as: $Min \sum_{i=1}^{n-1} LC_{E(V_i,V_{i+1})}$ for which $LC_{E(V_i,V_{i+1})} \geq 0$.

The data routing cost LC_E is computed based on the factors like (i) $E_{C(V_i,V_j)}$, which is transmission energy consumed over link (i,j) (ii) $E_{T(V_i)}$, which is available total energy (including harvested, battery and gained energy

through RF transfer) of node i, (iii) $E_{T(V_j)}$, which is available energy (including harvested, battery and gained energy through RF transfer) of node j. $E_{C(V_i,V_j)}$ can be calculated by (1). Each CH in the virtual ring discovers its potential neighbors through which it can gain energy over RF energy transfer mechanism. In this scheme, we transmit the energy alongside the data in our routing process to compensate for the transmission energy consumed over each link. It is pertinent to mention that more energy is conserved than consumed in terms of transmissions since sensor nodes are transferring the energy alongside the data by transmitting a strong signal, thus balancing out the incurred overhead for the receiving node. Our data routing cost LC_E can be defined in (12) as:

$$LC_{E(V_i,V_j)} = \frac{E_{C(V_i,V_j)}}{(E_{T(V_i)} + E_{T(V_j)})} \quad (12)$$

A data set $D(S, N_S, W_v/S_v, F_{ST}, LC_E)$ is proposed which consists of source (S) address, neighboring node (N_S) addresses, working–sleeping cycle schedule (W_v/S_v), status transition frequencies (F_{ST}) and data routing cost (LC_E) of a node to each of its neighbors in each data collection period, to investigate the opportunistic node connection between sensor nodes based on data routing cost. First we need to compute the time-frequency parameter $TF_{V_iV_j}$ of link connectivity $L_{V_iV_j}$ which depends on the working time of adjacent sensor nodes, data collection duration of mobile sink, and status transition frequencies of adjacent sensor nodes. $TF_{V_iV_j}$ can be calculated in (13) and (14) as:

$$TF_{V_iV_j} = \left(\frac{F_{STV_i}}{F_{ST_{max}}} \times \frac{W_{V_i}}{T_{CP}}\right)\left(\frac{F_{STV_j}}{F_{ST_{max}}} \times \frac{W_{V_j}}{T_{CP}}\right) \quad (13)$$

$$TF_{V_iV_{SINK}} = \left(\frac{F_{STV_i}}{F_{ST_{max}}} \times \frac{W_{V_i}}{T_{CP}}\right)\left(W_{V_{SINK}}\right) \quad (14)$$

where F_{STi} and F_{STj} are the status transition frequencies of V_i and V_j, W_{Vi} and W_{Vj} are the working time of V_i and V_j, T_{CP} is the data collection duration of mobile sink, F_{STmax} is the max status transition frequency value obtained from sensor node undergoing maximum transitions during T_{CP}. It is assumed that mobile sink has unlimited power and it will always remain in working mode i.e. $W_{VSINK} = 1$. Keeping in view LC_E and $TF_{V_iV_j}$, our link connectivity function $L_{V_iV_j}$ and $L_{V_{SINK}V_i}$ in terms will be,

$$L_{V_iV_j} = \alpha LC_E(i,j) + (1 - \alpha)TF_{V_iV_j} \quad (15)$$

$$L_{V_iV_j} = \alpha\left(\frac{E_{C(V_i,V_j)}}{(E_{T(V_i)} + E_{T(V_j)})}\right) + (1 - \alpha)\left(\frac{F_{STV_i}}{F_{ST_{max}}} \times \frac{W_{V_i}}{T_{CP}}\right)\left(\frac{F_{STV_j}}{F_{ST_{max}}} \times \frac{W_{V_j}}{T_{CP}}\right) \quad (16)$$

$$L_{V_{SINK}V_i} = \alpha LC_E(SINK, i) + (1 - \alpha)TF_{V_{SINK}V_i} \quad (17)$$

$$L_{V_{SINK}V_i} = \alpha\left(\frac{E_{C(SINK,V_i)}}{(E_{T(SINK)} + E_{T(V_i)})}\right) + (1 - \alpha) \times \left(\frac{F_{STV_i}}{F_{ST_{max}}} \times \frac{W_{V_i}}{T_{CP}}\right) \quad (18)$$

where $LC_E(i, j)$ is the data routing cost associated with V_i and V_j, $LC_E(SINK, i)$ is the data routing cost between V_{SINK} and V_i respectively. α is the appropriate weight assigned to data routing cost and time-frequency parameter in (15) and (17). In order to realize the reliable data forwarding from any sensor node to mobile sink, we need to find optimal path. The product of link connectivity between adjacent sensor nodes along the path towards mobile sink or CH can be treated as Path Connectivity (PC). We have utilized the spanning tree algorithm to compute the optimal path using maximum value of path connectivity [45]. Mobile sink produces a spanning tree incorporating each node's path connectivity values and then broadcast this information in the network using R_L. PC between V_i and V_j can be formulated in (19) as:

$$PC_{V_iV_j} = PC_{V_iV_{i+t}} = \prod_{k=0}^{t-1} L_{V_{i+k}V_{i+(k+1)}} \quad (19)$$

Likewise, PC for V_i (neighboring node) of mobile sink V_{SINK} can be calculated as $PC_{V_{SINK}V_i} = L_{V_{SINK}V_i}$. Similarly, the PC of V_j (neighboring node of V_i) to V_{SINK} can be computed as $PC_{V_{SINK}V_j} = L^*_{V_{SINK}V_i}L_{V_iV_j}$ for which, $PATH(V_{SINK}, V_j, *) = \{V_{SINK}, V_j, 2\} = \{V_{SINK}, V_i, V_j\}$. Furthermore, if V_j is not directly connected to V_i, then the PC of V_j to V_{SINK} can be formulated as $PC_{V_{SINK}V_j} = PC^*_{V_{SINK}V_i}\prod_{k=0}^{t-1} L_{V_{i+k}V_{i+(k+1)}}$ where $V_{i+t} = V_j$ and in that case, $PATH(V_{SINK}, V_j, *) = \{V_{SINK}, V_j, t + 1\} = \{V_{SINK}, V_i, \ldots V_{i+t-1}, V_j\}$. Contrary to it, if V_j which is deployed just outside R_L need to communicate with mobile sink, then PC of V_j with V_{SINK} would depend on 3 factors i.e. (i) PC between V_{SINK} and its neighboring node, (ii) PC between V_{SINK} neighbor and V_{CH} (iii) PC between V_{CH} and its neighbor V_j located outside R_L.

$$PC_{V_{SINK}V_j^{RL}} = PC_{V_{SINK}V_i} * PC_{V_iV_{CH}} * PC_{V_{CH}V_j^{RL}} \quad (20)$$

$$PC_{V_{SINK}V_j^{RL}} = L_{V_{SINK}V_i} * \prod_{k=0}^{t-2} L_{V_{i+k}V_{i+(k+1)}} * L_{V_{i+(t-1)}V_{CH}} * L_{V_{CH}V_j^{RL}} \quad (21)$$

$$PATH\left(V_{SINK}, V_j^{RL}, *\right) = \left\{V_{SINK}, V_j^{RL}, t + 1\right\} = \{V_{SINK}, V_i, \ldots V_{i+t-1}, V_{CH}, V_j^{RL}\} \quad (22)$$

where $PC_{V_{SINK}V_i}$ is the path connectivity from neighboring node V_i to mobile sink, $PC_{V_iV_{CH}}$ is the path connectivity from V_i to V_{CH} and $PC_{V_{CH}V_j^{RL}}$ is the path connectivity from V_{CH} to its neighbor V_j located outside R_L in (20). If V_j is not directly connected with V_{CH}, then the PC of V_{SINK} with V_j outside R_L would be,

$$PC_{V_{SINK}V_j^{RL}}$$
$$= L_{V_{SINK}V_i} * \prod_{k=0}^{t-2} L_{V_{i+k}V_{i+(k+1)}} * L_{V_{i+(t-1)}V_{CH}}$$
$$* \prod_{k=0}^{u-2} L_{V_{CH+k}V_{CH+(k+1)}} * L_{V_{CH+(u-1)}V_j^{RL}} \quad (23)$$

Algorithm 3 HESTOR Energy Transfer Based Opportunistic Routing

---

Input:
1.　　　Virtual Ring around mobile sink
2.　　　Formation of data set $D(S, N_S, W_v/S_v, F_{ST}, R_E, B_S, LQF)$
3.　　　Formation of clusters in the virtual ring

Output:
4.　　　Optimal path connectivity towards mobile sink

Begin:
5.　　**if** node.location $=$ inside R_L, **then**
6.　　　　　Determine link connectivity　using $L_{V_{SINK}V_i} = \alpha LC_E(SINK, i) + (1 - \alpha)TF_{V_{SINK}V_i}$
7.　　　　　Determine path connectivity for neighbor V_i of V_{SINK} i.e. $PC_{V_{SINK}V_i} = L_{V_{SINK}V_i}$
8.　　　　**for** each node V_j inside R_L, **do**
9.　　　　　　**if** (V_j is directly connected to neighboring node V_i of V_{SINK}), **then**
10.　　　　　　　$PC_{V_{SINK}V_j} = L_{V_{SINK}V_i} * L_{V_iV_j}$
11.　　　　　　　$PATH(V_{SINK}, V_j, *) = \{V_{SINK}, V_j, 2\} = \{V_{SINK}, V_i, V_j\}$
12.　　　　　**else if** (V_j is a CH which is not connected to neighboring node V_i of V_{SINK}), **then**
13.　　　　　　　$PC_{V_{SINK}V_j} = PC_{V_{SINK}V_i} * \prod_{k=0}^{t-1} L_{V_{i+k}V_{i+(k+1)}}$ where$V_{i+t} = V_j$
14.　　　　　　　$PATH(V_{SINK}, V_j, *) = \{V_{SINK}, V_j, t+1\} = \{V_{SINK}, V_i, \ldots V_{i+t-1}, V_j\}$
15.　　　　　　**else**　$PC_{V_{SINK}V_j} = 0$
16.　　　　　　　$PATH(V_{SINK}, V_j, *) = \emptyset$
17.　　　　　**end if**
18.　　　**end for**
19.　　**else if** node.location $=$ outside R_L, **then**
20.　　　　　Determine link connectivity of adjacent nodes: $L_{V_iV_j} = \alpha LC_E(i, j) + (1 - \alpha)TF_{V_iV_j}$
21.　　　　**for** each node V_j outside R_L, **do**
22.　　　　　i **f** (V_j outside R_L is directly connected to any V_{CH}), **then**
23.　　　　　　Determine path connectivity from V_{CH} to V_j^{RL} i.e. $PC_{V_{CH}V_j^{RL}} = L_{V_{CH}V_j^{RL}}$
24.　　　　　　**if** $\{EOH_i < Q\}$, **then**
25.　　　　　　　$PC_{V_{SINK}V_j^{RL}} = PC_{V_{SINK}V_i} * \prod_{k=0}^{t-2} L_{V_{i+k}V_{i+(k+1)}} * PC_{V_{i+(t-1)}V_{CH}} * PC_{V_{CH}V_j^{RL}}$
26.　　　　　　　$PATH(V_{SINK}, V_j^{RL}, *) = \{V_{SINK}, V_j^{RL}, t+2\} = \{V_{SINK}, V_i, \ldots V_{CH}, V_j^{RL}\}$
27.　　　　　　**end if**
28.　　　　　**else if** (V_j is not directly connected to V_{CH}), **then**
29.　　　　　　$PC_{V_{CH}V_j^{RL}} = \prod_{k=0}^{t-1} L_{V_{CH+k}V_{CH+(k+1)}}$ where$V_{CH+t} = V_j^{RL}$
30.　　　　　　**if** $\{EOH_i < Q\}$, **then**
31.　　　　　　　$PC_{V_{SINK}V_j^{RL}} = PC_{V_{SINK}V_i} * \prod_{k=0}^{t-2} L_{V_{i+k}V_{i+(k+1)}} * PC_{V_{i+(t-1)}V_{CH}} * PC_{V_{CH}V_j^{RL}}$
32.　　　　　　　$PATH(V_{SINK}, V_j^{RL}, *) = \{V_{SINK}, V_j^{RL}, t+u\} = \{V_{SINK}, V_i, \ldots .V_{CH}, \ldots .V_j^{RL}\}$
33.　　　　　　**end if**
34.　　　　　**end if**
35.　　　　**end for**
36.　　**end if**

$$PATH\left(V_{SINK}, V_j^{RL}, *\right)$$
$$= \left\{V_{SINK}, V_j^{RL}, t+u\right\}$$
$$= \{V_{SINK}, V_i, \ldots . . V_{i+t-1}, V_{CH}, \ldots . V_{CH+(u-1)}, V_j^{RL}\}$$
$$\tag{24}$$

Here we have assumed that $V_j^{RL} = V_{CH+u}$ in which u is the number of hops on the path from V_{CH} to V_j^{RL} and t is the number of hops on the path from V_{SINK} to V_{CH} for which $1 \leq t \leq N - 1$ and $1 \leq u \leq N - 1$ in (24). As we are dealing with opportunistic node connections, so we have devised a mechanism for updating PC values after every round of

communication. The PC value is updated after comparing it with the previous PC values and selecting the maximum PC value among them, thus improving the efficiency of finding an optimal path as indicated by (25) and (26). The energy transfer based opportunistic routing process is summarized in Algorithm 3.

$$PC_{V_{SINK}V_j^{RL}}^{updated}$$
$$= max\left(PC_{V_{SINK}V_j^{RL}}, L_{V_{SINK}V_i} * \prod_{k=0}^{t-2} L_{V_{i+k}V_{i+(k+1)}}\right.$$
$$\left. *L_{V_{i+(t-1)}V_{CH}} * \prod_{k=0}^{u-2} L_{V_{CH+k}V_{CH+(k+1)}} * L_{V_{CH+(u-1)}V_j^{RL}}\right)$$
$$\tag{25}$$

$$PATH(V_{SINK}, V_j^{RL}, *)$$
$$= \{V_{SINK}, V_j^{RL}, (t+u)^{upd}$$
$$= \{V_{SINK}, V_i, \dots V_{i+t-1}^{upd}, , V_{CH}^{upd}, \dots, V_{CH+(u^{upd}-1)}^{upd}, V_j^{RL}\}$$
$$(26)$$

After the selection of optimal paths, we need to define our main routing strategy for data transmission and reception purposes. The conventional opportunistic routing strategy only involves asynchronous working–sleeping cycle metric and probably results in failed link connection between sensor nodes due to unannounced transition (working to sleeping mode) of any forwarder node. In order to resolve this ambiguity, we need to carefully design the HESTOR routing strategy based on expected optimal hops (EOH) [45]. EOH is defined as the number of hops it takes to forward a probe message or data packet from any sensor node in the network to mobile sink while consuming minimum energy. EOH will be used to select those forwarders which lead to a reliable data transmission between the source node and mobile sink while keeping the energy consumption as low and delay as minimum as possible. EOH also helps us in selecting the nodes in inner search space only when forwarding the packet from sensor node to mobile sink whereas selecting the nodes in outer search space only when forwarding the packet from mobile sink to any sensor node. Having received the RSSI which would estimate the distance between mobile sink and any sensor node, we can compute the EOH of each neighbor of a sensor node and compare the average EOH value against each of its neighbor's EOH value to make sure that the packet is forwarded to mobile sink using inner search space and packet if forwarded to a sensor node (away from mobile sink) using outer search space areas. Our objective for defining inner search space and outer search space areas is to achieve a balance between hop count and energy efficiency while forwarding the sensed data towards mobile sink.

$$EOH = \{EOH_1, EOH_2, EOH_3, \dots \dots EOH_n\} \quad (27)$$
$$Q = (EOH_1 + EOH_2 + EOH_3 + \dots + EOH_n)/n \quad (28)$$

where n is number of neighbors of a sensor node and Q is the average of EOH in (27) and (28). Our aim is to find the optimal path between sensor node and mobile sink, so we find the next hop based on maximum link connectivity between adjacent nodes. Energy harvesting approach in HESTOR leads to less unannounced transitions from working-sleeping mode and results in finding optimal path from any sensor node to mobile sink. After the mobile sink broadcasts the optimal and updated path information in the network, the data generating node sends an aggregation request packet towards virtual ring in order to acquire the position information of nearest CH from its CM i.e. RN or CN. Similarly, the CM forwards the aggregation reply packet to data generating node after receiving an aggregation request packet. The aggregation reply packet contains the address of nearest CH. We use inner search space mechanism for forwarding aggregation request packet and use outer search space mechanism for

forwarding aggregation reply packet as depicted from Fig. 7. Having received the aggregation reply packet, the source node extracts the address information of nearest CH and forwards the data packet to nearest CH using the optimal path. The CH receives multiple data packets from different sensor nodes, performs lossless data aggregation on those packets, concatenates multiple aggregated data packets into a single data packet of specified length and forwards that single data packet to mobile sink keeping in view the minimum delay and energy consumption constraints.
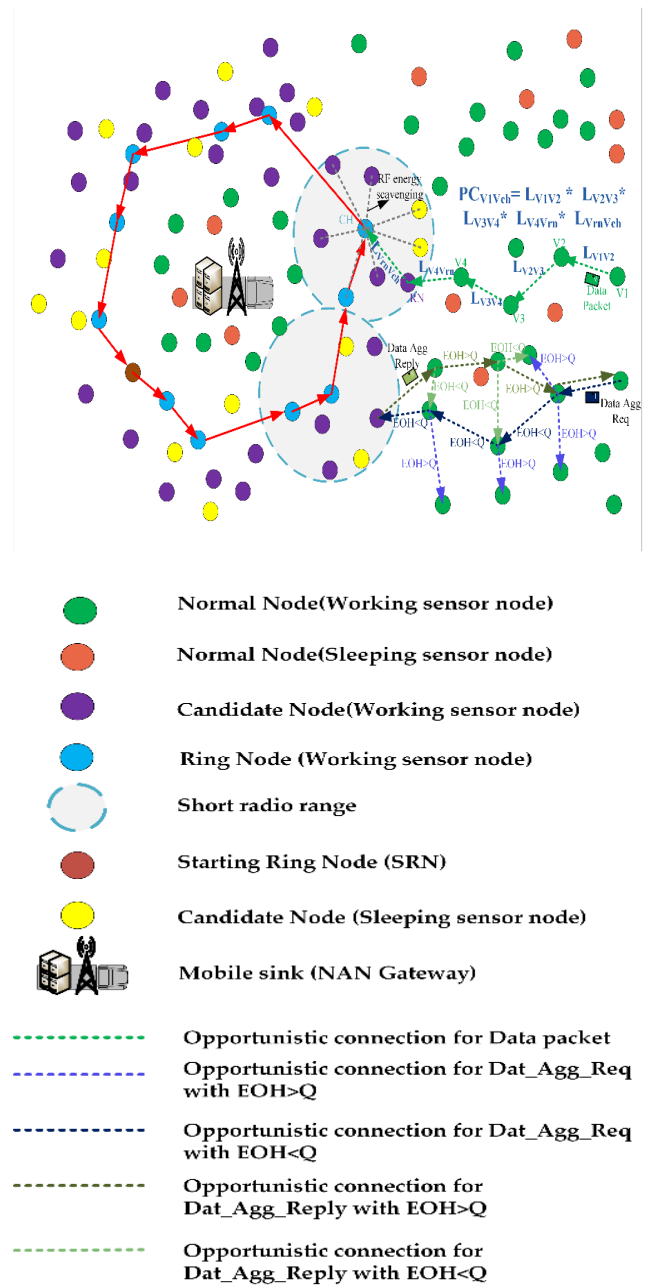

FIGURE 7. Agg_Req packet, Agg_Reply packet and Data packet forwarding.

Algorithm 4 Dat_Agg_Req Packet Arrives at **RN**

Input:
1. Optimal path connectivity towards mobile sink
Output:
2. Prepare Dat_Agg_Reply packet
Begin:
3.　**if** node.address　= Destination Address, **then**
4.　　**if** node.role = RN, **then**
5.　　　Create Dat_Agg_Reply packet
6.　　　Set address of its CH in Dat_Agg_Reply packet
7.　　　**if** data generating node V_j is in range of RN, **then**
8.　　　　Send Dat_Agg_Reply packet to V_j
9.　　　**else** determine the path connectivity of RN to source node and
10.　　　　then send Dat_agg_reply packet
11.　　　**end if**
12.　　**else if** node.role $\neq$ RN, **then**
13.　　　Determine the path connectivity of source node to RN and then
14.　　　send Dat_Agg_Req packet
15.　　**end if**
16.　**end if**

Algorithm 5 Dat_Agg_Reply Packet Arrives at Data Generating Node

---

Input:
1. Dat_Agg_Reply packet
Output:
2. Prepare Data packet
Begin:
3.　　　**if** node.address = data generating node Address, **then**
4.　　　　Check the address of V_{CH} and start preparing the data packet
5.　　　　Set total no. of aggregated packets as NADP in Data packet
6.　　　　**if** V_{CH} is in range of data generating node, **then**
7.　　　　　Send data packet to V_{CH}
8.　　　　**else**　Set V_{CH} address in Data packet
9.　　　　　Determine the path connectivity of data generating node to V_{CH}　and then
10.　　　　　send　the data packet
11.　　　　**end if**
12.　　　**else** determine path connectivity of RN to data generating node and　then send
13.　　　　Dat_agg_reply packet
14.　　　**end if**

As the CHs in the ring are responsible for operations like gathering, aggregating, transmitting to next-hop node and receiving data from prior nodes, we can say that the total energy consumed in virtual ring is proportional to energy consumed by all clusters in the virtual ring. Although CNs or cluster members of CHs also consume energy while sending the data or request packet to CHs but this amount of energy is less critical as compared to energy consumed by CHs [18]. The total energy consumed in a cluster of a virtual ring is the sum of energies consumed by all CMs in a cluster plus the energy consumed by their corresponding CH. The total energy consumed by a cluster $E_{cluster}$ is given in (29) as,

$$E_{cluster} = E_{CH} + \sum_{i=1}^{\left(\frac{N}{N_C}-1\right)} E_{CM_i} \qquad (29)$$

Furthermore, the total energy consumed by virtual ring can be expressed as:

$$E_{virtualring} = \sum_{j=1}^{N_C} E_{cluster_j} \qquad (30)$$

where N_C indicates the number of clusters in the virtual ring. The processing of aggregated data request packet and aggregated data reply packet are summarized in Algorithm 4 and 5. The processing of data packet at CH is given in Algorithm 6.

D. NETWORK MAINTENANCE

We need to maintain our virtual ring structure regularly to avoid network connectivity problems occurring due to disparities between energy consumption & overall end-end delay.

Algorithm 6 Processing Data Packet at CH

Input:
1. Data packet sent by data generating node
Output:
2. Forward the data packet to mobile sink
Begin:
3.　　　**if** node.address = V_{CH} address, **then**
4.　　　　　Receive and store aggregated data packet from data generating node
5.　　　　　V_{CH} aggregates all data packets by performing lossless data
6.　　　　　aggregation
7.　　　　　Forwards the aggregated data packet to mobile sink
8.　　　**else if** node.address ≠ V_{CH} address, then
9.　　　　　Determine the path connectivity of data generating node to V_{CH} and
10.　　　　　then send the data packet
11.　　　**end if**

Some of the significant features related to network maintenance are addressed in this section.

1) RE-CLUSTERING EPOCH

It is important to highlight that our network hierarchy should be changed if needed, in order to avoid saturating any CH in the ring and losing all the data packets forwarded towards that CH. This continues until selection of new CH in the next round. A pro-active approach is needed to avoid this bottleneck. The probe message sent by every sensor node to mobile sink contains working-sleeping cycle ad status transition frequency of that sensor node in specific data collection duration. This pro-active approach can prevent the loss of data packet. If the CH is about to undergo a transition, mobile sink is already aware of it and it assigns the best candidate among CMs of that CH to be the new CH, thus averting the loss of data packet. Furthermore, changing the network topology too frequent, will also lead towards an increase in the exchange of control packets, so re-clustering epoch of the network is always subject to trade-off i.e. re-clustering epoch should not be too large to avoid overburdening the CHs by enabling rotation of CH role in the ring. When re-clustering epoch is too large, the situation will lead towards unannounced and sudden transitions, therefore we need an appropriate value of re-clustering epoch to optimize the performance of clustering in the virtual ring.

2) RING ADJUSTMENT

We are well aware that RNs perform more energy consumable tasks than NNs. For a specific time of a day when solar harvested energy is not available and we have to rely on RF energy transfer, there is a possibility that the residual energy of most of the RNs is not sufficient enough to continue our network operations. Mobile sink takes the decision of adjusting the virtual ring in a way which could increase the network lifetime of HESTOR. The Although sink mobility could solve this problem as well but at the cost of increased control packet overhead and energy

consumption, so keeping in view the density of RNs and CNs, mobile sink performs the ring adjustment. The role of RN is interchanged with NN or CN depending on the type of ring adjustment. In HESTOR, we have two kinds of ring adjustments i.e. (i) Contraction Stage (ii) Expansion Stage.

For our ring to be successfully adjusted without any hindrances, we have marked two threshold boundaries i.e. R_S and R_L. The virtual ring can contract until it reaches R_S of mobile sink whereas the virtual ring can expand until it reaches R_L. In contraction stage, the number of RNs will be reduced to half in comparison to the current state which means less number of RNs will be engaged in advertising the CHs information to NNs but in expansion stage, the number of RNs will be doubled in comparison to current state which means that more number of RNs will be required to advertise the CH position information to NNs. The I_R and O_R are adjusted as per (31) and (32) respectively.

$$Expansion\ Stage : \begin{cases} newI_R = oldO_R \\ newO_R = oldO_R + (oldO_R - oldI_R) \end{cases}$$
$$(31)$$

$$Contraction\ Stage : \begin{cases} newO_R = oldI_R \\ newI_R = oldI_R - (oldO_R - oldI_R) \end{cases}$$
$$(32)$$

V. PACKET OVERHEAD CALCULATION

In HESTOR, each CH acquires the integrated sensed data from its CMs or NNs and then forwards the aggregated data to mobile sink. In our scheme, the network load is balanced during CH rotation in successive rounds of communication and by random movement of sink node. Let us assume that we have O(NW) exchanged packets as an overhead in which NW is the number of working sensor nodes in the network. If we assume that N_C is the number of CHs per round and N_{VR} is the number of nodes in the virtual ring, then we can calculate the overhead packets as:

- NW-1 packets used to send probe message to mobile sink
- NW-1 packets used for sending updated path information to mobile sink
- NW-N_{VR} packets used for sending aggregating reques
- NW-N_{VR} packets used for sending aggregating repl
- NW-N_C packets used for sending data packet to CH from any working nod
- N_C packets used for sending data packet from CH to mobile sink
- $\frac{N_{VR}}{N_C}$ packets used to multicast energy_req message to all CNs and RNs in the cluste
- $\frac{N_{VR}}{N_C}$ packets used to CH_Announce_message to CMs
- $\frac{N_{VR}}{N_C}$ -1 packets used to send connection request (Con_Req) to CHs.
- NW-1 packets received by all working nodes for link connectivity and path connectivity computation.

Therefore, the overhead of HESTOR will be O(NW) as $N_C \ll \frac{N_{VR}}{N_C} \ll$ NW.

VI. RESULTS

A. SIMULATION ENVIRONMENT

We have evaluated the performance of HESTOR in OMNET ++ and MATLAB 2019b using cross platform library (MEX-API) for simulating WSNs. This Application Programming Interface (API) can provide the user an easy bidirectional connection interface between MATLAB and OMNET++. We have utilized low rate, low cost, short range, flexible and low power consumption standard IEEE 802.15.4 for our PHY and MAC layer. The energy model defined in IEEE 802.15.4 is used to compute the energy consumed during data transmission, reception and sensing. In addition to it, we have also utilized the IEEE 802.15.4 MAC Layer specifications for data rate and data packet size. The performance metrics like control packet overhead, energy consumption, end-to-end delay, PDR, network lifetime and throughput are analyzed against two parametric benchmarks viz. sink mobility speed and node density. For sink mobility simulation, we have considered 1-15 km/h range while keeping the node density as constant i.e. 400 whereas for node density simulation, we have considered 300-500 rage as different number of heterogeneous sensor nodes while keeping the sink mobility speed as constant i.e. 5 km/h. Different sink mobility and node densities values are chosen to capture the performance of HESTOR in different circumstances i.e. dense network, sparse network, frequent re-clustering, ring adjustment etc. Our network operates in outdoor environment and the solar cells equipped with each sensor nodes harvests energy during the day. A typical solar cell generates 100 m/cm2, with conversion efficiency of 15which gives us the available ambient energy of 15 mW/cm2 in sunny conditions and the same reduces to 0.15 mW/cm2 due to clouds [66]. Other simulation parameters are summarized in Table 3. To evaluate the performance of HESTOR, we compared it with four different benchmarks: 1) VGB [32], 2) Ring Routing [10], 3) LBRR [30], 4) DA-EEORR [11]. It is pertinent to mention

TABLE 3. Simulation parameters.

Parameters	Values
Network Area (M × M)	800 m × 800 m
No. of sensor nodes in network (N)	300-500
Mobility Pattern	Randomly
Duration of a data collection duration	200 s
Weights α, α_1, β_1	0.8, 0.2, 1
η	0.4
μ	0.5
E_{elec}	50×10^{-9} J/bit
ε_{fs}	10×10^{-12} J/bit/m^2
ε_{mp}	0.0013×10^{-12} J/bit/m^4
Energy consumed during aggregation E_A	5×10^{-9} J/bit
Energy consumed by CH during data fusion	5×10^{-12} J/bit
Probe message size	70 bits
Lossless aggregated data packet size	127 bytes
Dat_Agg_Req packet size	45 bits
Dat_Agg_Reply packet size	70 bits
Transmission power of sensor node	−1 dBm
Initial energy of sensor node	60 J
MAC layer	IEEE 802.15.4
Initial ring formation radius IR and OR	75 m and 150 m
Data rate	250 Kbps
Receiver sensitivity	-85dBm @ 2.45GHz
Packet service rate	150 packets/s
Sink mobility speed	1, 5, 10, 15 km/h
Ring change period	600 s
Simulation time	2500 s

that the individual simulation results are the average over 25 runs and the length of each run is 2500 sec. The results stayed within −8of the sample mean when subjected to 95% confidence interval.

B. PERFORMANCE COMPARISON

The effect of various parameters on the performance of HESTOR and other existing benchmarks are provided in this section.

1) CONTROL PACKET OVERHEAD

The total energy consumed by sensor nodes during transmission and reception of control packets can be treated as control packet overhead. This metric is considered as overhead because of extra burden over the network as the exchange messages in terms of control packets do not contain sensed data and are only used for proper handling of data packets. Fig 8 depicts the energy consumed in terms of control packet against variable node density for VGB, ring routing, LBRR, DA-EEORR and HESTOR. At low node density, DA-EEORR and HESTOR perform better than VGB, ring routing & LBRR whereas at high node density, HESTOR outperforms all other protocols due to several reasons i.e. i) optimum number of RNs selected for virtual ring, ii) virtual ring CH election, iii) energy transfer based opportunistic routing. The performance of ring routing is better than LBRR for high node density due to the reason that more energy is consumed due to reception of AAPI packets by large number of neighbors at each hop. At low node densities, VGB performs better than ring routing and LBRR due to fixed number
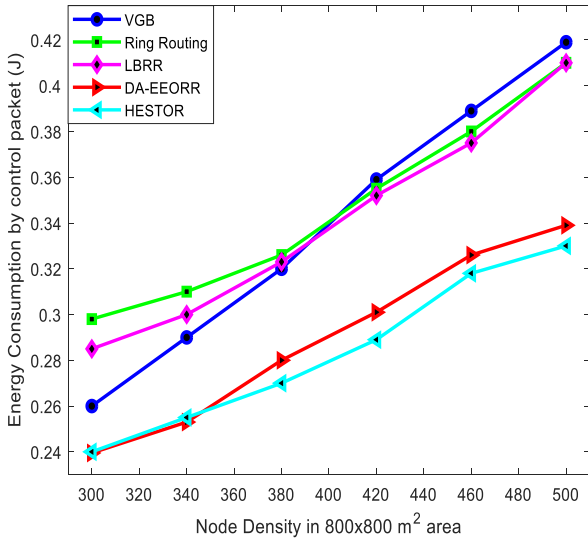
FIGURE 8. Energy consumption in terms of control packet overhead against variable node density.
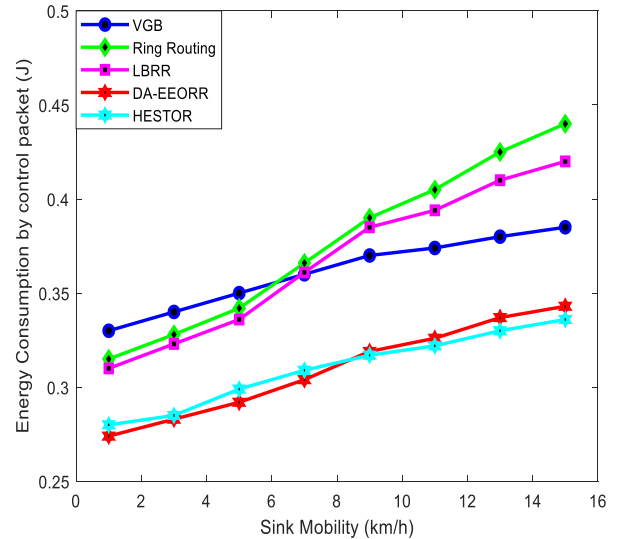

FIGURE 9. Energy consumption in terms of control packet overhead against sink mobility.

of grid-header nodes which ensures minimum control packet overhead but for higher node density, those fixed grid-header nodes against variable RNs in ring routing and LBRR result in slightly higher overhead.

Fig 9 illustrates the control packet overhead of VGB, ring routing, LBRR, DA-EEORR and HESTOR against variable sink mobility. At low sink mobility, HESTOR and DA-EEORR performs better than VGB, ring routing and LBRR due to reduced number of AAPI and RAPI control packets but for higher sink mobility, HESTOR outperforms all other protocols. LBRR follows the same pattern as ring routing for all sink mobility speeds but performs slightly better than ring routing due to formation of initial ring in a single trial in LBRR. At higher sink mobility speeds, optimum number of RNs selected in DA-EEORR for advertisement of mobile sin's position results in minimization of exchange messages in comparison to VGB, ring routing and LBRR. Both DA-EEORR and HESTOR don't have to relay their control packets to multi-hop away anchor nodes and their opportunistic routing strategy is based on optimal path connectivity calculation. DA-EEORR performs slightly better than HESTOR at low sink mobility speeds due to the reason of CH elections and formation of clusters in the ring in HESTOR. At higher sink mobility speeds, lack of energy harvesting feature in DA-EEORR results in sudden transition of already energy exhausted RN_{maxRE}, thus leading to a situation where a new RN_{maxRE} is required for which the control packet overhead will definitely increase. Our proposed scheme HESTOR is designed to use the energy scavenging abilities to provide support to energy exhausted CHs in the ring, thus performing better than DA-EEORR for higher sink mobility speeds.

2) ENERGY CONSUMPTION
It can be calculated as the total energy consumed in the network during data transmission, reception, sensing,

aggregation and relaying functions. Fig 10 depicts the total energy consumption of VGB, ring routing, LBRR, DA-EEORR and HESTOR for different sink mobility speeds. The performance behavior of all protocols in Fig 10 is analogous at different sink mobility speeds i.e. energy consumption increases with the increase in sink mobility speed. HESTOR and DA-EEORR outperforms all other protocols due to aggregation of multiple data packets into a single packet of specified length which helps in reducing the overall energy consumption. Moreover, the performance differences between DA-EEORR and HESTOR in terms of overall energy consumption are due to i) virtual CH elections, ii) creation of virtual clusters in the ring, iii) energy transfer based opportunistic routing. Furthermore, the possibility of a sudden transition of RN_{maxRE} node in DA-EEORR would
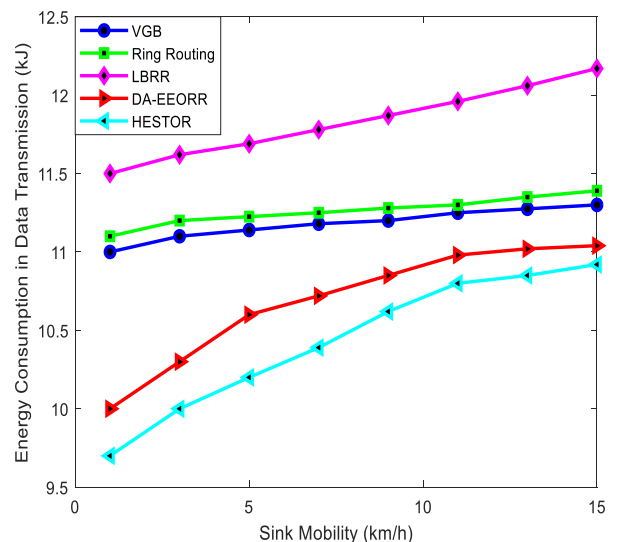

FIGURE 10. Energy consumed during data transmission against sink mobility speed.

require the aggregation request packets and data packets to be re-routed to another RN_{maxRE} which would result in an increase in energy consumption in DA-EEORR. Our proposed scheme HESTOR is associated with harvesting energy scavenging abilities in order to avoid such kind of sudden transitions from working to sleep mode.

Fig 11 illustrates the comparison of total energy consumption (sensing, transmission and reception) for data transmission with that of energy consumed in terms of control packet overhead for different network maintenance frequencies. It is quite obvious from the Fig 10 that the energy consumed for data transmission is quite higher than that of energy consumed in terms of control packet overhead. In addition to it, the network maintenance frequency or re-clustering epoch i.e. 1/1, 1/6, 1/12, 1/18 and 1/24 means to adjust the virtual ring in terms of expansion or contraction in every round, once in 6 rounds, once in 12 rounds, once in 18 rounds and once in 24 rounds respectively. Both total energy consumption and energy consumed in terms of control packet overhead graphs indicate that the best performance is achieved when the network is maintained in every round because the energy consuming functions of virtual CHs in the ring are suitably rotated among all cluster members. However, increasing the network maintenance frequency results in the overall increase of total energy consumption and energy consumed in terms of control packet overhead.
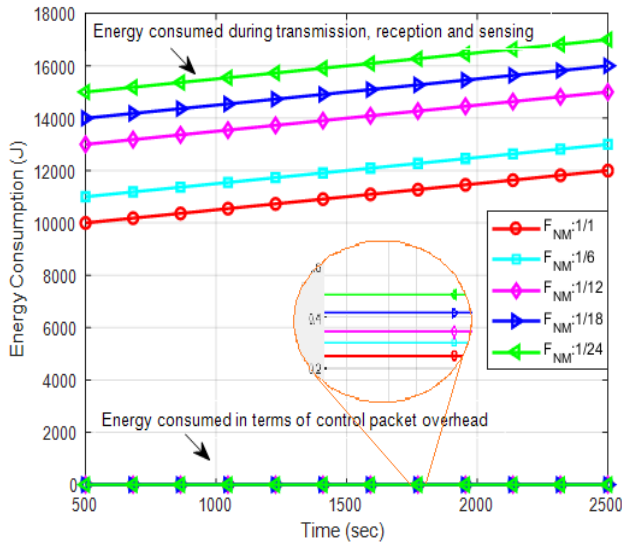
FIGURE 11. Energy consumption in terms of overhead and data transmission with different epochs against simulation time.

3) NETWORK LIFETIME

Network lifetime can be defined as the time difference when the simulation starts till the first sensor node dies (no residual energy left to perform sensing, transmission, reception, aggregation etc.), some percentage of sensor nodes die or all sensor nodes die. It can also be defined in terms of loss of coverage or when the network is partitioned due to non-existence

of path from source to mobile sink node [17], [67]. In this article, two such time intervals have been considered i.e. i) first sensor node dies (FND) and ii) half of the sensor node die (HND). Fig 12 shows the stacked grouped bar chart to illustrate the significance of FND and HND for VGB, ring routing, LBRR, DA-EEORR and HESTOR against variable node density. Due to single anchor node usage for advertising mobile sink position information, ring routing shows degraded performance against all other routing protocols for all values of node density. The selection of multiple RN_{maxRE} in DA-EEORR and multiple clusters in HESTOR results in better performance against different node densities. The higher number of grid-header nodes used for updating sink's position in VGB for higher node densities leads to decreased network lifetime due to increase in energy consumption.

Fig 13 shows the stacked grouped bar chart of network lifetime for VGB, ring routing, LBRR, DA-EEORR and HESTOR against different sink mobility speeds. Even at low sink mobility speed, ring routing depicts degraded performance due to single anchor node handling all the data traffic towards mobile sink, thus becoming the cause of FND in the network. However, at higher sink mobility speed, VGB performance is worse than ring routing due to the fact that data transmission path from source to mobile sink is not always energy efficient, thus resulting in poor performance especially with respect to HND. The selection of multiple RN_{maxRE} in DA-EEORR and multiple clusters in HESTOR results in better performance against different sink mobility speeds. The absence of harvested energy, lack of energy transfer based on opportunistic routing and overburdening of RN_{maxRE} in DA-EEORR leads to better performance of HESTOR over DA-EEORR. Moreover, the CHs in the ring receive energy along with the data from RNs or CNs through RF links, which also play a significant role in improving the network lifetime of HESTOR.

Live nodes metric reflect the average number of live nodes per round. A live node is the one whose energy supply is not fully depleted. Fig 14 depicts the number of live nodes in HESTOR for different network maintenance frequencies. As the network maintenance frequency increases, the number of live nodes in HESTOR increases as well. If the re-clustering epoch or network maintenance frequency is low, there is a possibility that some sensor nodes especially CH consumed more energy than it receives through harvesting or energy transfer mechanism, thus resulting in the decreased live node count. Fig 15 shows the number of live nodes in HESTOR for different data sampling frequencies. The best result is achieved when data sampling frequency is low i.e. high live node count at Fs = 0.01 but when the data sampling frequency is high, HESTOR demonstrates low live node count. We can observe from Fig. that 60% of the sensor nodes are alive when data sampling frequency Fs = 2 i.e. data sampling time is $2 \times 3600 = 7200$ times per hour. In addition to it, if Fs is large and the node density is low (increasing distance between sensor nodes), then the energy consumed by a distant apart CH would be quite more than the sum of
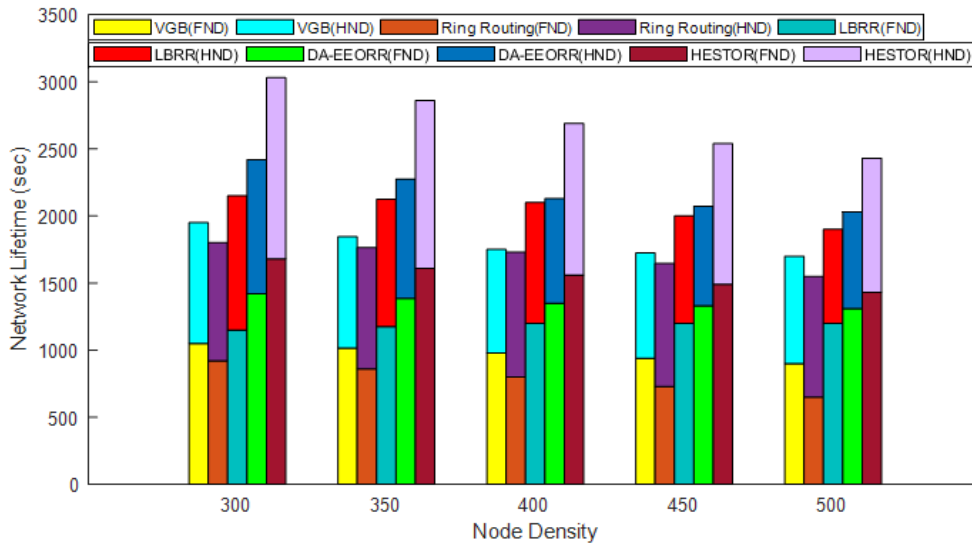
FIGURE 12. Network Lifetime in terms of FND and HND against node density.
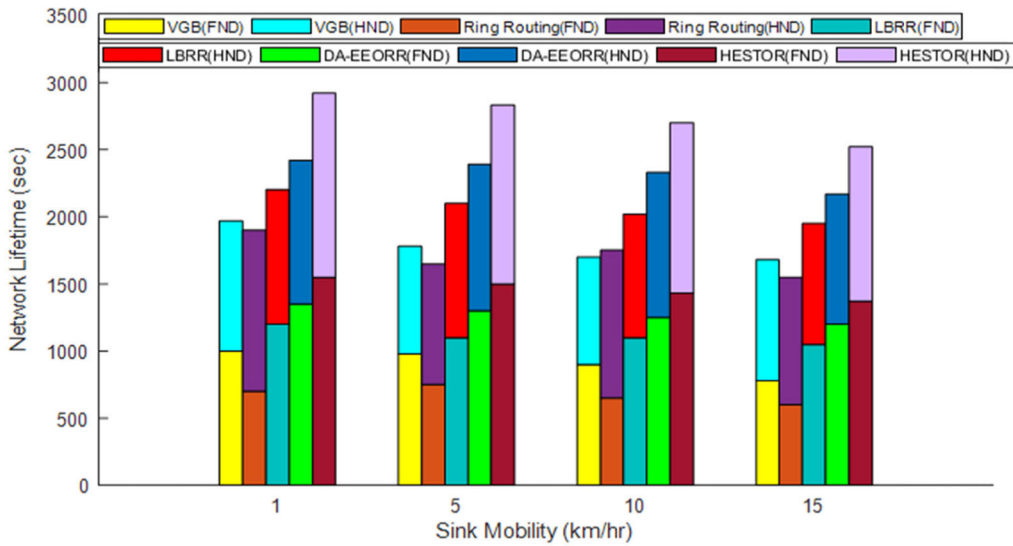

FIGURE 13. Network Lifetime in terms of FND and HND against sink mobility speed.

energy being harvested and received through energy transfer, hence resulting in low live node count.

4) HOP COUNT
Fig 15 shows the increase in hop count of HESTOR against the increase in network density for different values of re-clustering epoch. It is evident that the hop counts for low re-clustering epoch are higher than the hop counts for other re-clustering epochs and also, the hop counts for high re-clustering epoch are lower than the hop counts for all other re-clustering epochs or network maintenance frequencies. It means regularly maintain our network will lead to lower hop count and seldom changing to our network would result in increased hop counts. The nodes near the mobile sink are

overburdened due to traffic convergence, so regular network maintenance is required in HESTOR to keep the hop count as low as possible. Low hop count also means low processing and queuing delay, hence resulting in lower avg. end-end delay.

5) PACKET DELIVERY RATIO (PDR)
Higher network reliability can be reflected by higher number of successfully received packets at the mobile sink. The protocols like VGB, ring routing and LBRR in which aggregation is not performed, PDR can be defined as the ratio of successfully received data packets at mobile sink to total data packets sent by all sensor nodes but for protocols like DA-EEORR and HESTOR, PDR can be defined
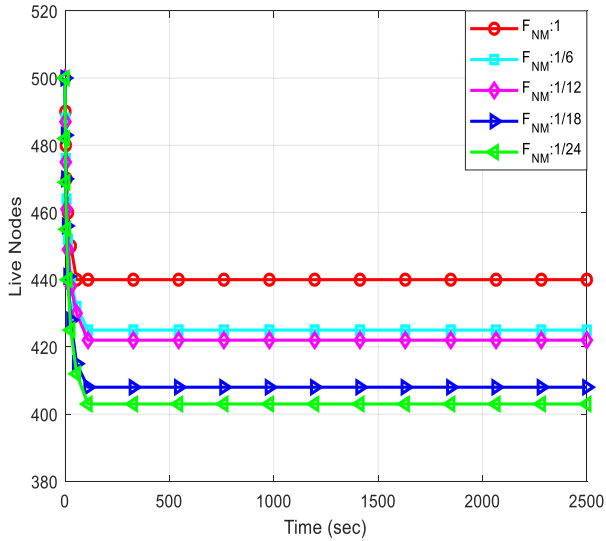
FIGURE 14. Live nodes with different epochs against simulation time.
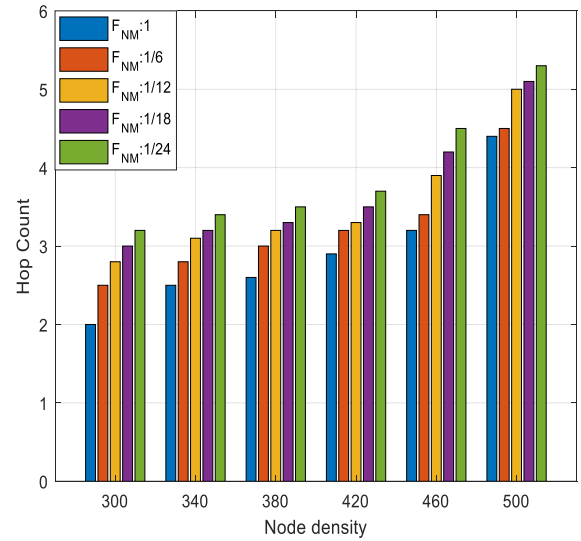
FIGURE 16. Hop count with different re-clustering epochs against node density.
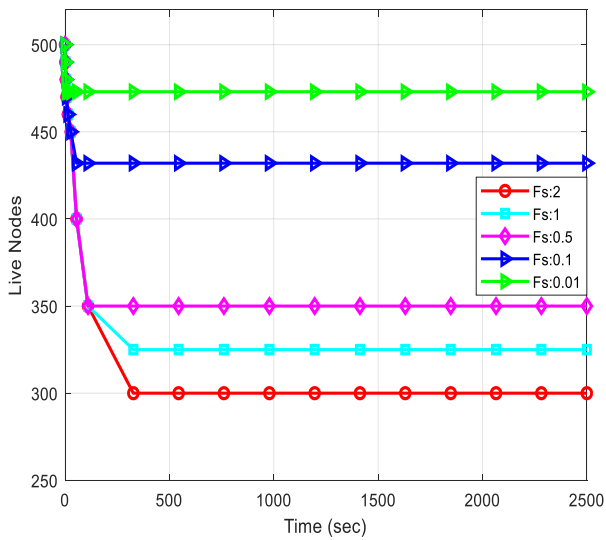

FIGURE 15. Live nodes with different sampling frequencies against simulation time.
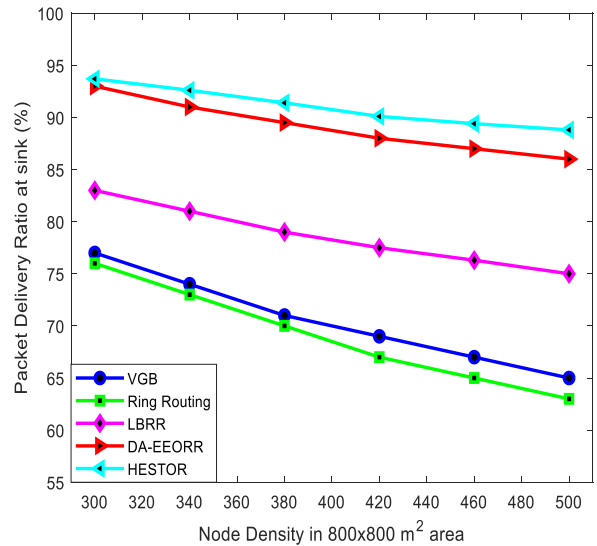

FIGURE 17. Packet delivery ratio against variable node density.

as the ratio of successfully received aggregated data packets to total data packets generated by all sensor nodes. Fig 17 demonstrates the PDR of VGB, ring routing, LBRR, DA-EEORR and HESTOR against different node densities. For all values of node density, ring routing depicts poor performance and HESTOR outperforms all other routing protocols. VGB is slightly better than ring routing but still its performance deteriorates due to data packet collision with advertisement packet especially when number of sensor nodes are increased in the network. Although the chances of packet collision is reduced in DA-EEORR due to data aggregation feature but the sudden transition of RN_{maxRE} might result in loss of packets at mobile sink. Our proposed scheme HESTOR is designed to avoid such failures in DA-EEORR by providing enough energy to CHs and successfully changing

the network maintenance frequency for better performance in terms of PDR.

Fig 18 shows the performance of VGB, ring routing, LBRR, DA-EEORR and HESTOR against variable sink mobility. Ring routing shows degraded performance at low sink mobility due to single anchor node which couldn't handle all the data traffic single handedly. Ring routing shows an improvement in PDR with increase in sink mobility due to better collision avoidance but again shows degraded performance due to an increase in control packet overhead. VGB performs slightly better than ring routing at low sink mobility speeds but shows poor performance against other protocols due to frequent sink position advertisement by grid-header nodes. At higher sink mobility speed, the PDR of VGB drops due to increased probability of packet collision with sink position advertisement packet. LBRR with multiple anchor nodes
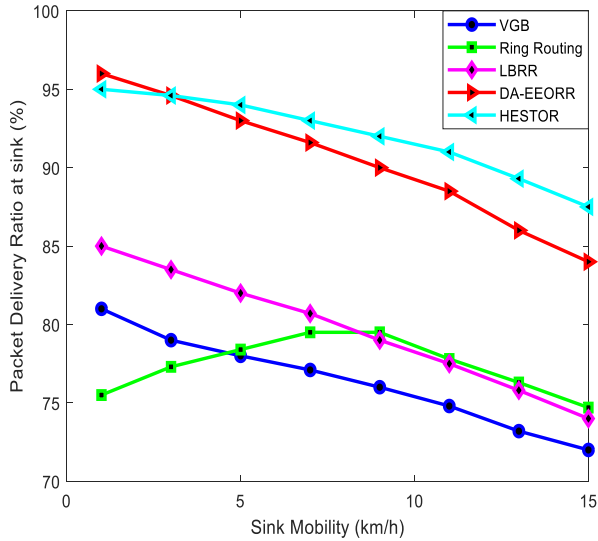
FIGURE 18. Packet delivery ratio against variable sink mobility speed.

FIGURE 19. Packet delivery ratio with different re-clustering epochs against node density.

FIGURE 20. Packet delivery ratio with different sampling frequencies against node density.

results in better PDR than ring routing and VGB. The PDR of DA-EEORR is better than VGB, ring routing and LBRR as it avoids packet collision problem by assigning TDMA slots to each RN_{maxRE} for data transmission. HESTOR ensures that CHs in the ring are rotated by changing the network maintenance frequency and also supports data aggregation by every CH which reduces the number of transmitted data packets to mobile sink and results in better PDR than all other protocols especially at higher sink mobility speeds.

Fig 19 shows PDR of HESTOR against variable node density values for different network maintenance frequencies. It is evident from Fig 19 that changing the network maintenance frequency in every round leads to higher PDR in comparison to scenarios in which network maintenance frequency is changed after 6 rounds, 12 rounds, 18 rounds and 24 rounds. This occurs due to adjustment of ring in terms of expansion or contraction and rotation of CH roles among different nodes in the ring which further helps our design in achieving load balancing. Fig 20 depicts the effect of sampling frequency on PDR of HESTOR against different node density values. We have chosen 5 different sampling frequencies to demonstrate their effect on performance metrics. We have selected the range of Fs as 0.01 ∼ 2 which means that data sampling is performed $0.01 \times 3600 = 36$ times per hour when Fs = 0.01, and $2 \times 3600 = 7200$ times per hour when Fs = 2. The best and worst patterns of PDR are achieved for Fs = 2 and Fs = 0.01 respectively which means PDR increases with the increase in data sampling frequency and decreases with the corresponding decrease in sampling frequency.

6) AVERAGE END-END DELAY

Average end-end delay can be defined as average time between generation of data packet at source node and reception of the data packet at BS including the queuing delay and processing delay. Fig 21 exhibits the avg. end-end delay
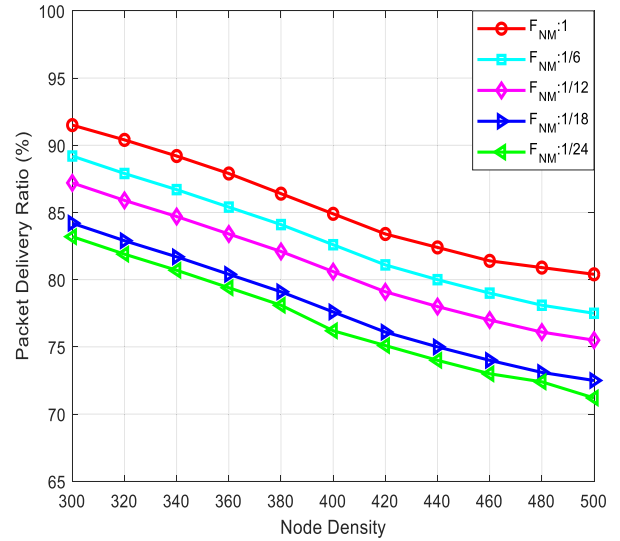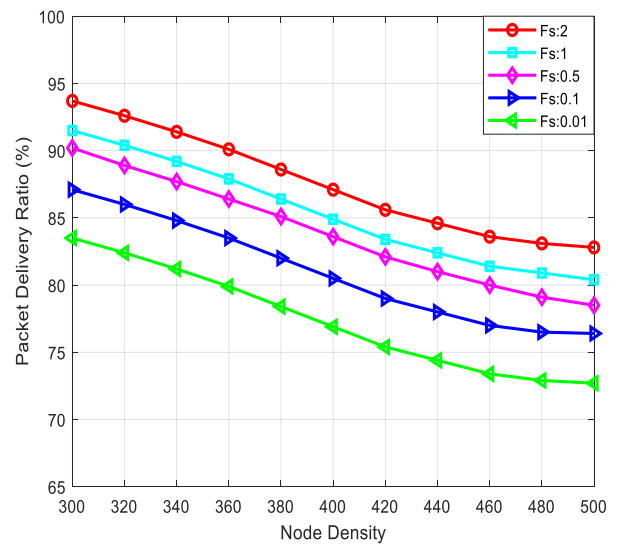
of VGB, ring routing, LBRR, DA-EEORR and HESTOR against different node density values. The end-end delay of VGB is quite low as whereas LBRR shows worst performance in comparison to other protocols. The selection of highest energy next-hop node in every round in LBRR results in the increased path length from source node to mobile sink, thus increasing the hop count and resulting in more avg. end-end delay. HESTOR approaches VGB when the node density value reaches 480. This performance is achieved due to higher probability of finding energy-efficient and delay aware opportunistic next-hop node in the inner search space towards mobile sink.

Fig 22 depicts the performance of VGB, ring routing, LBRR, DA-EEORR and HESTOR in terms of avg. end-end delay against variable sink mobility speed. Again, LBRR
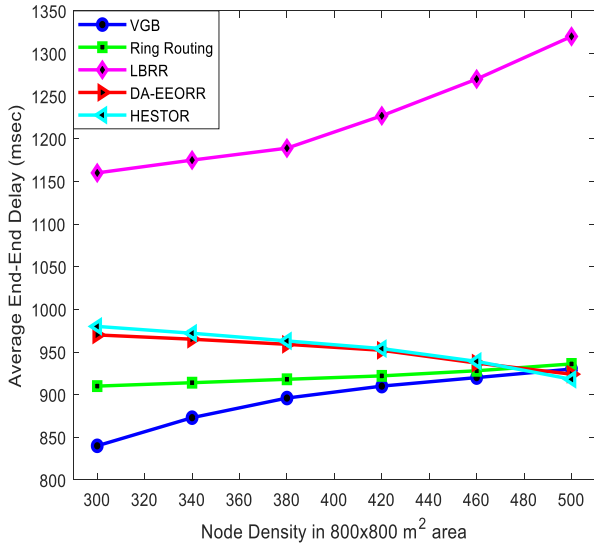
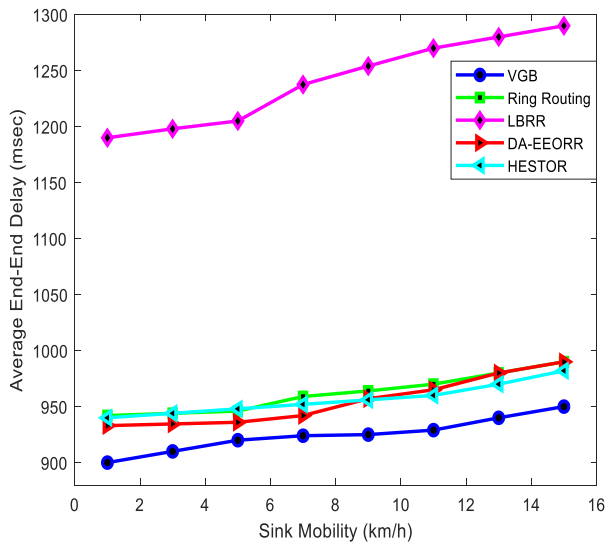**FIGURE 21. Average end-end-delay against node density.**

FIGURE 22. Average end-end-delay against variable sink mobility speed.

shows degraded performance due to increased path length from source to mobile sink and VGB shows best performance in comparison to all other protocols. VGB achieves low delay due to frequent acquisition of sink's position from grid-header nodes. In HESTOR, we have introduced the concept of EOH which helps our proposed scheme in achieving relatively better avg. end-end delay against ring routing and LBRR throughout and against DA-EEORR when sink mobility reaches 9 km/h. DA-EEORR and HESTOR's performance in comparison to VGB is low due to the reason that it takes higher amount of time to acquire the sink position when the limits of ring contraction and expansion are reached.

7) THROUGHPUT

Throughput can be defined as the measure of average number of data packets reaching BS (or mobile sink) per round. Fig 23 depicts the throughput of HESTOR for different
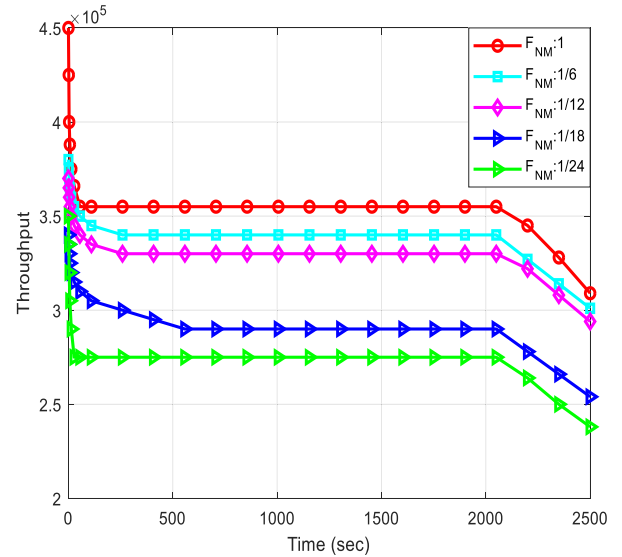

FIGURE 23. Throughput with different re-clustering epochs against simulation time.
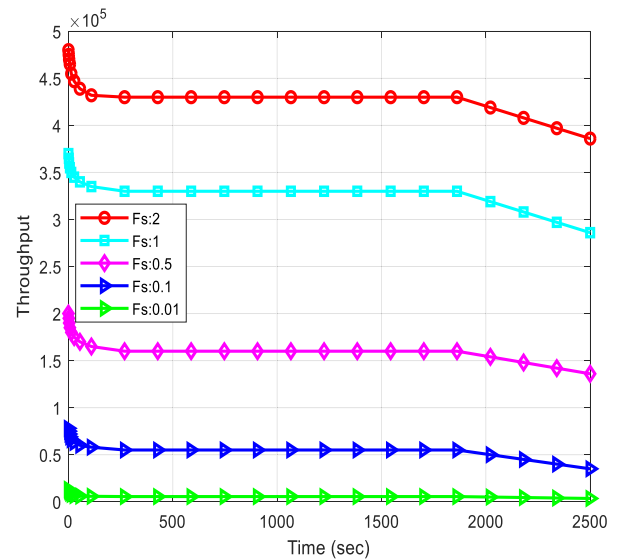

FIGURE 24. Throughput with different sampling frequencies against simulation time.

network maintenance frequencies. It is obvious from the Fig. 23 that as the re-clustering epoch increases, the throughput grows as well. Similarly, the throughput decreases when the re-clustering epoch is small. The best throughput is achieved when re-clustering epoch is once in every round and the worst throughput is due to re-clustering epoch as once in 24 rounds. Fig. 24 illustrates the throughput against simulation time for different values of data sampling frequency. The best results are obtained when data sampling frequency is very high. Likewise, the worst throughput is achieved when data sampling frequency is low i.e. data sampling time is $0.01 \times 3600 = 36$ times per hour. It is pertinent to mention that the energy consumption of a sensor node has a direct relationship with the distance between source and sink.

If Fs is large and distance between source and sink is also large due to sparsely populated network, then a sensor node would consume more energy than it can possibly harvest or received from its neighbors. This is the reason why some nodes die at the beginning of the simulation when Fs is high.

VII. CONCLUSION

In this paper, a novel, distributed, HESTOR protocol is proposed which opts to solve the energy replenishment and control packet overhead problems in EHWSNs through a dynamic network architecture involving a hybrid (ring + cluster) topology. The formation of a virtual ring and the two-tier clustering approach as an overlay reflects the reliability and longevity of WSN when supported with energy harvesting sources. The CH competition in each cluster is based on the criteria of energy harvesting potential of sensor nodes. Moreover, CHs in virtual ring are used for the advertisement of mobile sink current position as well as for forwarding aggregated data towards mobile sink using energy transfer based opportunistic routing algorithm. The energy transfer based opportunistic routing algorithm is developed to route data and energy simultaneously by following optimal path connectivity, hence extending the network lifetime of EHWSN. The effectiveness of HESTOR is confirmed after carefully analyzing and evaluating its performance against several existing benchmarks. The simulation results have clearly shown that employing the hybrid topology of HESTOR results in the improvement of energy consumption, control packet overhead, network lifetime, packet delivery ratio and average end-end delay. The possible future work would be to alter the hybridization of several hierarchical routing topologies and to incorporate energy based opportunistic routing in them.

REFERENCES

[1] M. Hefeeda and M. Bagheri, "Wireless sensor networks for early detection of forest fires," in *Proc. IEEE Internatonal Conf. Mobile Adhoc Sensor Syst.*, Oct. 2007, pp. 1–6, doi: 10.1109/mobhoc.2007.4428702.

[2] F. T. Jaigirdar and M. M. Islam, "A new cost-effective approach for battlefield surveillance in wireless sensor networks," in *Proc. Int. Conf. Netw. Syst. Secur. (NSysS)*, Jan. 2016, pp. 1–6.

[3] E. Hamida and G. Chelius, "Strategies for data dissemination to mobile sinks in wireless sensor networks," *IEEE Wireless Commun.*, vol. 15, no. 6, pp. 31–37, Dec. 2008.

[4] D. Chen, Z. Liu, L. Wang, M. Dou, J. Chen, and H. Li, "Natural disaster monitoring with wireless sensor networks: A case study of data-intensive applications upon low-cost scalable systems," *Mobile Netw. Appl.*, vol. 18, no. 5, pp. 651–663, Oct. 2013.

[5] F. Ye, G. Zhong, S. Lu, and L. Zhang, "Gradient broadcast: A robust data delivery protocol for large scale sensor networks," *Wireless Netw.*, vol. 11, no. 3, pp. 285–298, 2005, doi: 10.1007/s11276-005-6612-9.

[6] K. Kweon, H. Ghim, J. Hong, and H. Yoon, "Grid-based energy-efficient routing from multiple sources to multiple mobile sinks in wireless sensor networks," in *Proc. 4th Int. Symp. Wireless Pervas. Comput.*, Melbourne, VIC, Australia, Feb. 2009, pp. 1–5, doi: 10.1109/iswpc.2009.4800585.

[7] V. Safdar, F. Bashir, Z. Hamid, H. Afzal, and J. Y. Pyun, "A hybrid routing protocol for wireless sensor networks with mobile sinks," in *Proc. ISWPC*, Jul. 2012, pp. 1–5, doi: 10.1109/iswpc.2012.6263665.

[8] W. Y. Poe and J. B. Schmitt, "Placing multiple sinks in time-sensitive wireless sensor networks using a genetic algorithm," in *Proc. 14th GI/ITG Conf.-Meas., Modelling Evaluation Comput. Commun. Syst.*, Dortmund, Germany, Mar./Apr. 2008, pp. 1–15.

[9] S. Maurya, V. K. Jain, and D. R. Chowdhury, "Delay aware energy efficient reliable routing for data transmission in heterogeneous mobile sink wireless sensor network," *J. Netw. Comput. Appl.*, vol. 144, pp. 118–137, Oct. 2019, doi: 10.1016/j.jnca.2019.06.012.

[10] C. Tunca, S. Isik, M. Y. Donmez, and C. Ersoy, "Ring routing: An energy-efficient routing protocol for wireless sensor networks with a mobile sink," *IEEE Trans. Mobile Comput.*, vol. 14, no. 9, pp. 1947–1960, Sep. 2015.

[11] J. Anees, H.-C. Zhang, B. G. Lougou, S. Baig, and Y. G. Dessie, "Delay aware energy-efficient opportunistic node selection in restricted routing," *Comput. Netw.*, vol. 181, Nov. 2020, Art. no. 107536, doi: 10.1016/j.comnet.2020.107536.

[12] A. Cammarano, C. Petrioli, and D. Spenza, "Pro-energy: A novel energy prediction model for solar and wind energy-harvesting wireless sensor networks," in *Proc. IEEE 9th Int. Conf. Mobile Ad-Hoc Sensor Syst. (MASS)*, Las Vegas, NV, USA, Oct. 2012, pp. 75–83, doi: 10.1109/MASS.2012.6502504.

[13] D. Porcarelli, D. Spenza, D. Brunelli, A. Cammarano, C. Petrioli, and L. Benini, "Adaptive rectifier driven by power intake predictors for wind energy harvesting sensor networks," *IEEE J. Emerg. Sel. Topics Power Electron.*, vol. 3, no. 2, pp. 471–482, Jun. 2015, doi: 10.1109/JESTPE.2014.2316527.

[14] A. Kansal, J. Hsu, S. Zahedi, and M. B. Srivastava, "Power management in energy harvesting sensor networks," *ACM Trans. Embedded Comput. Syst.*, vol. 6, p. 32, Sep. 2007, doi: 10.1145/1274858.1274870.

[15] S. Sudevalayam and P. Kulkarni, "Energy harvesting sensor nodes: Survey and implications," *IEEE Commun. Surveys Tuts.*, vol. 13, no. 3, pp. 443–461, 3rd Quart., 2011, doi: 10.1109/SURV.2011.060710.00094.

[16] M. M. Afsar and M.-H. Tayarani-N, "Clustering in sensor networks: A literature survey," *J. Netw. Comput. Appl.*, vol. 46, pp. 198–226, Nov. 2014.

[17] J. Anees, H.-C. Zhang, S. Baig, B. Guene Lougou, and T. G. Robert Bona, "Hesitant fuzzy entropy-based opportunistic clustering and data fusion algorithm for heterogeneous wireless sensor networks," *Sensors*, vol. 20, no. 3, p. 913, Feb. 2020, doi: 10.3390/s20030913.

[18] M. M. Afsar and M. Younis, "A load-balanced cross-layer design for energy-harvesting sensor networks," *J. Netw. Comput. Appl.*, vol. 145, Nov. 2019, Art. no. 102390, doi: 10.1016/j.jnca.2019.06.010.

[19] D. Priya, Haripriya, and Kulothungan, "An energy efficient link stability based routing scheme for wireless sensor networks," in *Proc. Int. Conf. Commun. Signal Process. (ICCSP)*, Chennai, India, Apr. 2017, pp. 6–8, doi: 10.1109/iccsp.2017.8286711.

[20] G. Yang, Z. Peng, and X. He, "Data collection based on opportunistic node connections in wireless sensor networks," *Sensors*, vol. 18, no. 11, p. 3697, Oct. 2018, doi: 10.3390/s18113697.

[21] J. Luo, J. Hu, D. Wu, and R. Li, "Opportunistic routing algorithm for relay node selection in wireless sensor networks," *IEEE Trans. Ind. Informat.*, vol. 11, no. 1, pp. 112–121, Feb. 2015, doi: 10.1109/TII.2014.2374071.

[22] A. Boukerche and A. Darehshoorzadeh, "Opportunistic routing in wireless networks: Models, algorithms, and classifications," *ACM Comput. Surv.*, vol. 47, no. 2, pp. 1–36, Jan. 2015, doi: 10.1145/2635675.

[23] F. K. Shaikh and S. Zeadally, "Energy harvesting in wireless sensor networks: A comprehensive review," *Renew. Sustain. Energy Rev.*, vol. 55, pp. 1041–1054, Mar. 2016, doi: 10.1016/j.rser.2015.11.010.

[24] F. Deng, X. Yue, X. Fan, S. Guan, Y. Xu, and J. Chen, "Multisource energy harvesting system for a wireless sensor network node in the field environment," *IEEE Internet Things J.*, vol. 6, no. 1, pp. 918–927, Feb. 2019, doi: 10.1109/JIOT.2018.2865431.

[25] D. Brunelli, C. Moser, L. Thiele, and L. Benini, "Design of a solar-harvesting circuit for batteryless embedded systems," *IEEE Trans. Circuits Syst. I, Reg. Papers*, vol. 56, no. 11, pp. 2519–2528, Nov. 2009, doi: 10.1109/TCSI.2009.2015690.

[26] J. Jeong, X. Jiang, and D. Culler, "Design and analysis of micro-solar power systems for wireless sensor networks," in *Proc. 5th Int. Conf. Networked Sens. Syst.*, IKanazawa, Japan, Jun. 2008, pp. 181–188, doi: 10.1109/INSS.2008.4610922.

[27] S. Solanki, V. Singh, and P. K. Upadhyay, "RF energy harvesting in hybrid two-way relaying systems with hardware impairments," *IEEE Trans. Veh. Technol.*, vol. 68, no. 12, pp. 11792–11805, Dec. 2019, doi: 10.1109/TVT.2019.2944248.

[28] M. Sansoy, A. S. Buttar, and R. Goyal, "Empowering wireless sensor networks with RF energy harvesting," in *Proc. 7th Int. Conf. Signal Process. Integr. Netw. (SPIN)*, Noida, India, Feb. 2020, pp. 273–277, doi: 10.1109/SPIN48934.2020.9071376.

[29] C. Tunca, S. Isik, M. Y. Donmez, and C. Ersoy, "Distributed mobile sink routing for wireless sensor networks: A survey," *IEEE Commun. Surveys Tuts.*, vol. 16, no. 2, pp. 877–897, 2nd Quart., 2014, doi: 10.1109/surv.2013.100113.00293.

[30] S. Maurya, V. Gupta, and V. K. Jain, "LBRR: Load balanced ring routing protocol for heterogeneous sensor networks with sink mobility," in *Proc. IEEE Wireless Commun. Netw. Conf. (WCNC)*, San Francisco, CA, USA, Mar. 2017, pp. 1–6, doi: 10.1109/WCNC.2017.7925728.

[31] A. W. Khan, A. H. Abdullah, M. A. Razzaque, J. I. Bangash, and A. Altameem, "VGDD: A virtual grid based data dissemination scheme for wireless sensor networks with mobile sink," *Int. J. Distrib. Sensor Netw.*, vol. 11, no. 2, Feb. 2015, Art. no. 890348, doi: 10.1155/2015/890348.

[32] R. Yarinezhad and A. Sarabi, "Reducing delay and energy consumption in wireless sensor networks by making virtual grid infrastructure and using mobile sink," *AEU-Int. J. Electron. Commun.*, vol. 84, pp. 144–152, Feb. 2018.

[33] A. T. Erman, A. Dilo, and P. Havinga, "A virtual infrastructure based on honeycomb tessellation for data dissemination in multi-sink mobile wireless sensor networks," *EURASIP J. Wireless Commun. Netw.*, vol. 2012, no. 1, pp. 1–27, Dec. 2012, doi: 10.1186/1687-1499-2012-17.

[34] S.-W. Han, I.-S. Jeong, and S.-H. Kang, "Low latency and energy efficient routing tree for wireless sensor networks with multiple mobile sinks," *J. Netw. Comput. Appl.*, vol. 36, no. 1, pp. 156–166, Jan. 2013.

[35] S. Sharma and S. K. Jena, "Data dissemination protocol for mobile sink in wireless sensor networks," *J. Comput. Eng.*, vol. 2014, pp. 1–10, Apr. 2014, doi: 10.1155/2014/560675.

[36] S. Sharma, D. Puthal, S. K. Jena, A. Y. Zomaya, and R. Ranjan, "Rendezvous based routing protocol for wireless sensor networks with mobile sink," *J. Supercomput.*, vol. 73, no. 3, pp. 1168–1188, Mar. 2017, doi: 10.1007/s11227-016-1801-0.

[37] A. Hawbani, X. Wang, H. Kuhlani, S. Karmoshi, R. Ghoul, Y. Sharabi, and E. Torbosh, "Sink-oriented tree based data dissemination protocol for mobile sinks wireless sensor networks," *Wireless Netw.*, vol. 24, no. 7, pp. 2723–2734, Oct. 2018, doi: 10.1007/s11276-017-1497-y.

[38] A. Muthu Krishnan and P. Ganesh Kumar, "An effective clustering approach with data aggregation using multiple mobile sinks for heterogeneous WSN," *Wireless Pers. Commun.*, vol. 90, no. 2, pp. 423–434, Sep. 2016, doi: 10.1007/s11277-015-2998-6.

[39] M. Cardei and Y. Yang, "Delay-constrained energy-efficient routing in heterogeneous wireless sensor networks," *Int. J. Sensor Netw.*, vol. 7, no. 4, pp. 236–247, 2010, doi: 10.1504/ijsnet.2010.033207.

[40] C. Konstantopoulos, G. Pantziou, N. Vathis, V. Nakos, and D. Gavalas, "Efficient mobile sink-based data gathering in wireless sensor networks with guaranteed delay," in *Proc. 12th ACM Int. Symp. Mobility Manage. Wireless Access (MobiWac)*, 2014, pp. 47–54, doi: 10.1145/2642668.2642674.

[41] C. Konstantopoulos, N. Vathis, G. Pantziou, and D. Gavalas, "Employing mobile elements for delay-constrained data gathering in WSNs," *Comput. Netw.*, vol. 135, pp. 108–131, Apr. 2018, doi: 10.1016/j.comnet.2018.02.007.

[42] E. B. Hamida and G. Chelius, "A line-based data dissemination protocol for wireless sensor networks with mobile sink," in *Proc. IEEE Int. Conf. Commun.*, May 2008, pp. 2201–2205, doi: 10.1109/icc.2008.420.

[43] M. A. Habib, S. Saha, M. A. Razzaque, M. Mamun-or-Rashid, G. Fortino, and M. M. Hassan, "Starfish routing for sensor networks with mobile sink," *J. Netw. Comput. Appl.*, vol. 123, pp. 11–22, Dec. 2018, doi: 10.1016/j.jnca.2018.08.016.

[44] V. T. Venkateswarlu, P. V. Naganjaneyulu, and D. N. Rao, "Delay sensitive data routing optimization using rendezvous agents in wireless sensor networks with mobile sink," *Int. J. Comput. Appl.*, pp. 1–8, Feb. 2019, doi: 10.1080/1206212x.2019.1576326.

[45] Anees, Zhang, Baig, and Lougou, "Energy-efficient multi-disjoint path opportunistic node connection routing protocol in wireless sensor networks for smart grids," *Sensors*, vol. 19, no. 17, p. 3789, Sep. 2019, doi: 10.3390/s19173789.

[46] Z. H. Mir and Y.-B. Ko, "A quadtree-based hierarchical data dissemination for mobile sensor networks," *Telecommun. Syst.*, vol. 36, nos. 1–3, pp. 117–128, Nov. 2007, doi: 10.1007/s11235-007-9062-0.

[47] S. M. Bozorgi, M. G. Amiri, A. S. Rostami, and F. Mohanna, "A novel dynamic multi-hop clustering protocol based on renewable energy for energy-harvesting wireless sensor networks," in *Proc. 2nd Int. Conf. Knowl.-Based Eng. Innov. (KBEI)*, Nov. 2015, pp. 619–624, doi: 10.1109/KBEI.2015.7436116.

[48] P. Zhang, G. Xiao, and H.-P. Tan, "Clustering algorithms for maximizing the lifetime of wireless sensor networks with energy-harvesting sensors," *Comput. Netw.*, vol. 57, no. 14, pp. 2689–2704, Oct. 2013, doi: 10.1016/j.comnet.2013.06.003.

[49] S. Peng, T. Wang, and C. P. Low, "Energy neutral clustering for energy harvesting wireless sensors networks," *Ad Hoc Netw.*, vol. 28, pp. 1–16, May 2015, doi: 10.1016/j.adhoc.2015.01.004.

[50] J. Li and D. Liu, "DPSO-based clustering routing algorithm for energy-harvesting wireless sensor networks," in *Proc. Int. Conf. Wireless Commun. Signal Process. (WCSP)*, 2015, pp. 1–5.

[51] J. Bai, M. Fan, J. Yang, Y. Sun, and C. Phillips, "Smart energy harvesting routing protocol for WSN based E-Health systems," in *Proc. Workshop Pervas. Wireless Healthcare*, New York, NY, USA, Jun. 2015, pp. 23–28, doi: 10.1145/2757290.2757296.

[52] G. Martinez, S. Li, and C. Zhou, "Wastage-aware routing in energy-harvesting wireless sensor networks," *IEEE Sensors J.*, vol. 14, no. 9, pp. 2967–2974, Sep. 2014, doi: 10.1109/JSEN.2014.2319741.

[53] S. Padakandla, K. J. Prabuchandran, and S. Bhatnagar, "Energy sharing for multiple sensor nodes with finite buffers," *IEEE Trans. Commun.*, vol. 63, no. 5, pp. 1811–1823, May 2015.

[54] R. V. Prasad, S. Devasenapathy, V. S. Rao, and J. Vazifehdan, "Reincarnation in the ambiance: Devices and networks with energy harvesting," *IEEE Commun. Surveys Tuts.*, vol. 16, no. 1, pp. 195–213, 1st Quart., 2014.

[55] L. R. Varshney, "Transporting information and energy simultaneously," in *Proc. IEEE Int. Symp. Inf. Theory*, Toronto, ON, Canada, Jul. 2008, pp. 1612–1616, doi: 10.1109/ISIT.2008.4595260.

[56] S. Guo, F. Wang, Y. Yang, and B. Xiao, "Energy-efficient cooperative tfor simultaneous wireless information and power transfer in clustered wireless sensor networks," *IEEE Trans. Commun.*, vol. 63, no. 11, pp. 4405–4417, Nov. 2015, doi: 10.1109/TCOMM.2015.2478782.

[57] X. Zhou, R. Zhang, and C. K. Ho, "Wireless information and power transfer: Architecture design and rate-energy tradeoff," *IEEE Trans. Commun.*, vol. 61, no. 11, pp. 4754–4767, Nov. 2013, doi: 10.1109/TCOMM.2013.13.120855.

[58] H. Lin, Y. Guo, L. Huang, K. Ding, and Z. Li, "A body sensor network based on simultaneous wireless information and power transfer," in *Proc. IEEE 16th Int. Conf. Commun. Technol. (ICCT)*, Hangzhou, China, Oct. 2015, pp. 553–555, doi: 10.1109/ICCT.2015.7399899.

[59] T. D. Ponnimbaduge Perera, D. N. K. Jayakody, S. K. Sharma, S. Chatzinotas, and J. Li, "Simultaneous wireless information and power transfer (SWIPT): Recent advances and future challenges," *IEEE Commun. Surveys Tuts.*, vol. 20, no. 1, pp. 264–302, 1st Quart., 2018, doi: 10.1109/COMST.2017.2783901.

[60] Z. Hu, N. Wei, and Z. Zhang, "Optimal resource allocation for harvested energy maximization in wideband cognitive radio network with SWIPT," *IEEE Access*, vol. 5, pp. 23383–23394, 2017, doi: 10.1109/ACCESS.2017.2737034.

[61] G. Han, J. Jiang, C. Zhang, T. Q. Duong, M. Guizani, and G. K. Karagiannidis, "A survey on mobile anchor node assisted localization in wireless sensor networks," *IEEE Commun. Surveys Tuts.*, vol. 18, no. 3, pp. 2220–2243, 3rd Quart., 2016, doi: 10.1109/comst.2016.2544751.

[62] L. Karim, N. Nasser, and T. El Salti, "RELMA: A range free localization approach using mobile anchor node for wireless sensor networks," in *Proc. IEEE Global Telecommun. Conf. GLOBECOM*, Miami, FL, USA, Dec. 2010, pp. 1–5, doi: 10.1109/glocom.2010.5683802.

[63] A. Gopakumar and L. Jacob, "Localization in wireless sensor networks using particle swarm optimization," in *Proc. IET Conf. Wireless, Mobile Multimedia Netw.*, Beijing, China, 2008, pp. 227–230, doi: 10.1049/cp:20080185.

[64] X. Li, J. Yang, A. Nayak, and I. Stojmenovic, "Localized geographic routing to a mobile sink with guaranteed delivery in sensor networks," *IEEE J. Sel. Areas Commun.*, vol. 30, no. 9, pp. 1719–1729, Oct. 2012, doi: 10.1109/jsac.2012.121016.

[65] W. B. Heinzelman, A. P. Chandrakasan, and H. Balakrishnan, "An application-specific protocol architecture for wireless microsensor networks," *IEEE Trans. Wireless Commun.*, vol. 1, no. 4, pp. 660–670, Oct. 2002, doi: 10.1109/twc.2002.804190.

[66] S. Roundy, D. Steingart, L. Frechette, P. Wright, and J. Rabaey, "Power sources," *Wirel. Sensor Netw.*, vol. 2920, pp. 1–17, Mar. 2004.

[67] O. Ogundile and A. Alfa, "A survey on an energy-efficient and energy-balanced routing protocol for wireless sensor networks," *Sensors*, vol. 17, no. 5, p. 1084, May 2017, doi: 10.3390/s17051084.

JUNAID ANEES received the B.S. degree from the Institute of Space Technology, Islamabad, Pakistan, in 2010, and the M.S. degree in electrical engineering from COMSATS University Islamabad, Pakistan, in 2015. He is currently pursuing the Ph.D. degree with the School of Energy Science and Engineering, Harbin Institute of Technology, China. He is a Senior Manager in ground segment network operations with the Public Sector Organization, Pakistan. His research interests include energy harvesting wireless sensor networks, opportunistic routing, smart grids, distributed computing, cognitive radio sensor networks, and mobile networking.

HAO-CHUN ZHANG received the B.E., M.E., and Ph.D. degrees from the Harbin Institute of Technology (HIT), in 1999, 2001, and 2007, respectively. He is currently the Head of the Department of Nuclear Science and Engineering and an Executive Professor with the HIT-CORYS Nuclear System Simulation International Joint Research Center (Sino-France). He has about 150 research publications in peer reviewed journals and conferences, five books, and two translations of foreign books. Apart from the main research in the area of engineering thermo-physics, his current research interests include computational energy science, nuclear system simulation, and ultrasonic aircraft thermal protection.

BACHIROU GUENE LOUGOU received the Ph.D. degree from the Harbin Institute of Technology, China, in 2018.

He joined the faculty of Harbin Institute of Technology in 2018, where he is serving as a Research Scientist and an Assistant Professor. His research interests include carbon-neutral energy, hydrogen storage systems, CO2 utilization, heat and mass transfer, energy-efficient utilization, emission reduction, and advanced energy storage materials, including porous catalyst/redox materials.

SOBIA BAIG (Senior Member, IEEE) received the B.S. degree from the University of Engineering and Technology, Taxila, Pakistan, in 1995, and the master's and Ph.D. degrees in electronics engineering from the Ghulam Ishaq Khan Institute, Topi, Pakistan, in 2001 and 2008, respectively.

She is currently an Associate Professor with the Department of Electrical Engineering, COMSATS University Islamabad, Lahore, Pakistan. Her research interests include modulation techniques for 5G networks, smart grid communication techniques, multicarrier modulation techniques, application of wavelet-based modulation techniques in the wireline digital subscriber line (DSL), and power line communication (PLC) networks.

YABIBAL GETAHUN DESSIE received the B.S. degree from Bahir Dar University, Ethiopia, in 2005, and the M.S. degree in physics from Addis Ababa University, Ethiopia, in 2010. He is currently pursuing the Ph.D. degree with the School of Energy Science and Engineering, Harbin Institute of Technology, China. He is also the Director of science and technology with Public Sector Organization, Ethiopia. His research interests include energy harvesting, photovoltaic development, energy storage materials, environmental pollutants, and development of green energy.

YIYI LI received the B.S. degree from the China University of Petroleum (East China), Qingdao, China, in 2018. She is currently pursuing the Ph.D. degree with the School of Energy Science and Engineering, Harbin Institute of Technology, China. Her research interests include heat and mass transfer, metamaterials, intelligent energy manipulation, energy conversion, and thermodynamic.

● ● ●